DYNAMIC VISUAL PROCESSING: CREATING REPRESENTATIONS OF THE WORLD

by

ANGIE MOURAD MICHAIEL

A DISSERTATION

Presented to the Department of Biology
and the Graduate School of the University of Oregon
in partial fulfillment of the requirements
for the degree of
Doctor of Philosophy

December 2019

DISSERTATION APPROVAL PAGE

Student: Angie Mourad Michaiel

Title: Dynamic Visual Processing: Creating Representations of the World

This dissertation has been accepted and approved in partial fulfillment of the requirements for the Doctor of Philosophy degree in the Department of Biology by:

David McCormick	Chairperson
Cris Niell	Advisor
Michael Posner	Core Member
Santiago Jaramillo	Core Member
Matthew Smear	Institutional Representative

And

Kate Mondloch	Interim Vice Provost and Dean of the Graduate School

Original approval signatures are on file with the University of Oregon Graduate School.

Degree awarded December 2019

DISSERTATION ABSTRACT

Angie Mourad Michaiel

Doctor of Philosophy

Department of Biology

December 2019

Title: Dynamic Visual Processing: Creating Representations of the World

Vision is a vital sense upon which our experience of the world is built. Classical views of vision designate it as a purely feedforward process where external visual information from the environment is passively processed within the brain. More recent work has revealed that vision is more dynamic; the brain has the ability to also utilize information from internal representations of current and future goals, context, and learned expectations to build more adaptive perceptual representations and sensorimotor transformations. The aim of this dissertation is to examine vision in both the context of disrupted visual processing (i.e., altered internal representations) and goal directed visual behavior in order to understand the dynamic nature of vision.

In this thesis, I describe two dissimilar approaches to examine these different aspects of visual processing in the mammalian brain. In the first approach, covered in Chapter II, I describe experiments and results in which neural substrates known to mediate accurate visual perception were perturbed using a hallucinogenic compound that activates serotonin-2A receptors. Using multiple methods, we observed that agonizing this receptor subtype leads to a strong reduction in sensory-driven visual cortical activity,

potentially placing more reliance on internal representations and expectations of the world, which may work to generate hallucinations and sensory disruptions.

This first approach followed traditional methods of visual neurophysiology, in which mechanisms of visual processing were manipulated and observed in an unnatural but well controlled context. However, paradigms such as this dramatically limit natural exploration of the visual environment, which is naturally achieved through directed eye, head, and body movements. In Chapter III I will describe a system I designed to record bilateral eye movements while unrestrained mice perform a visually guided, goal directed behavior, capture of live insect prey. Utilizing this technique, we are beginning to understand the coordination of eye and head movements during active vision in the context of natural, goal-directed behavior. Here, I describe two opposing approaches to understand dynamic visual processing, ultimately answering longstanding questions about how the brain allows organisms to interact in their environments.

This dissertation includes previously published co-authored material.

CURRICULUM VITAE

NAME OF AUTHOR: Angie Mourad Michaiel

GRADUATE AND UNDERGRADUATE SCHOOLS ATTENDED:

University of Oregon, Eugene
University of California, Davis
University of Sussex, Brighton, UK

DEGREES AWARDED:

Doctor of Philosophy, 2019, University of Oregon
Bachelors of Science in Neurobiology, Physiology, and Behavior and Minor in Middle Eastern and South Asian Studies, 2012, University of California, Davis

AREAS OF SPECIAL INTEREST:

Neurobiology
Sensory Processing
Vision

PROFESSIONAL EXPERIENCE:

Junior Specialist, University of California, Davis, Center for Neuroscience, 01/2013– 07/2014

Undergraduate Research Assistant, University of California, Davis, 09/2009–03/2012

GRANTS, AWARDS, AND HONORS:

National Institute of Child Health and Human Development (2T32HD007348-26),
Serotonergic Modulation of Visual Processing, University of Oregon, 2015–2018

University of Oregon Department of Biology Diversity, Equity, and Inclusion Award 2019

Institute of Neuroscience, Neuroscience As Art Award, 2019

University of Oregon Graduate Forum, first place Panel Discussion Winner, June 2018

University of Oregon General University Scholarship, September 2018 – June 2019

University of Oregon Women in Graduate Sciences Travel Award, July 2017

University of Oregon Institute of Neuroscience Best Poster Award, September 2016

University of Oregon Promising Scholars Award, 2014 – Present

University of California Education Abroad Program Fellowship, 2011

PUBLICATIONS

A.M. Michaiel, P.R.L. Parker, C.M. Niell (2019). A Hallucinogenic Serotonin-2A Receptor Agonist Reduces Visual Response Gain and Alters Temporal Dynamics. *Cell Reports* 3475-3483

A.M. Michaiel, C.M. Niell (2019). Binocular Gaze Stabilization During Prey Capture in Mice. *In Preparation.*

ACKNOWLEDGEMENTS

I would first like to acknowledge my advisor, Dr. Cris Niell, for his guidance, and training throughout the years. He has helped me better myself scientifically, more than I imagined was possible. He has taught me that no experiment is ever completed and that there is no problem without a solution. Cris has always reacted with support, acknowledgement, and patience whenever I encounter an issue, and with joy and excitement when I have good news to share. Cris gave me the space to be creative with my work rather than being purely instructive. His work in creating an inclusive and friendly environment in the lab has undoubtedly been the source of my happiness during graduate school. I will be very sad to leave the lab.

I have been extremely lucky to have had wonderful mentors before and during my graduate career. I would like to thank Dr. Jennifer Hoy for her mentorship early in my graduate career. She has continued to be my mentor, primary role model, and friend; thank you for believing in me! Her excitability and success constantly inspires me. I would like to thank Dr. Phil Parker for being a great source of support and the best colleague and friend anyone could ask for. It was a pleasure to work with him on the serotonin project and I hope I get the privilege to work with him in the future; he has taught me so much about science and self-advocacy. Dr. Denise Niell has grown to be one of my dearest friends. Her infectious laughter and ability to transform negative situations to positive ones has kept me going. She is an incredible scientist, and a perfect friend. I'd like to thank Dr. Judit Pungor for being so compassionate and loving, from the first day we met.

I would like to thank members of the Niell lab, past and present, for their scientific discussions, understanding, acceptance of me, and our friendship: Mea Songco, Johanna Tomorsky, Ian Etherington, Mandi Severson, Elliott Abe, Dr. Joseph Wekselblatt, Kristen Chauvin, and Dr. Hannah Bishop. I have been so lucky to work in such an inclusive, lighthearted, and hardworking lab; I will definitely miss it.

Notably, I would like to thank and acknowledge the University of Oregon Womxn in Neuroscience group for their overwhelming support and passion, and their ability to empower each other in creative and inspiring ways. With Womxn in Neuroscience, I was able to practice identifying shared values within my community, become educated about factors that prevent inclusivity in communities, and devise actions towards mitigating issues related to gender and racial identities in science and in my community.

I especially would like to acknowledge my dog, Pluto, for bringing me joy and treating me with unconditional love every day, even when he is grumpy from eating too much cheese.

I would like to thank my partner, James Matonte, for his love and support for me. I am constantly in awe of his ability to push our growth as both individuals and as a unit, and as people who contribute to the empowerment of our communities; you empower me.

This work was supported in part by an Institutional Developmental Training Grant through the department of Biology, 2T32HD007348-26A1, and by the University of Oregon Promising Scholars Award.

I dedicate this work to my parents, Sameh and Samia Michaiel, for their endless sacrifices. Without leaving their homes in Egypt in search of personal, economic, religious, and political freedom, and without their tenacity in always striving for something better, I would not have the opportunity to pursue the luxury of scientific research or constantly revel in its beauty. I am immensely grateful for the freedoms their sacrifices have afforded me : they have given me the opportunity to not be complacent in my knowledge. Throughout my life, they encouraged me to pursue whichever interests I was attracted to with their repeated advice that success is built on three pillars: passion, dedication, and hard work. They encouraged my curiosity and love of animals and nature and didn't get too upset when I brought home bags of seashells or unplanned pets to do 'experiments' with.

I also dedicate this work to my two brothers and best friends in the world, Anthony and Jonathan Michaiel; they are my muses and I am so proud of them. Tony has a transcendent sense of empathy that has helped me feel supported throughout my life, and especially in the last few years as I have been separated from my family. I am proud of his creativity and motivation for finding beauty in even the darkest parts of life. Johny has always been a positive light in my life, constantly reminding me to see the bright side of any situation and continue the fight to live positively. Every problem is temporary to him, because he is able to move past it so quickly.

Finally, I would like to dedicate this work to my grandmother, Sophie Saddik Grace, who passed away during my time in graduate school. She was an angel who had no other motivation than to share love with others.

TABLE OF CONTENTS

LIST OF FIGURES

Figure Page

CHAPTER I

INTRODUCTION

Vision is a dynamic sense which evolved to allow organisms to survive in the face of changing environments. The first photosensitive proteins appeared roughly 1.5 million years ago in prokaryote bacteria and cyanobacteria which guided them to light where energy and nutrition could be found (Williams, 2016). Since then, vision has evolved even more profoundly complex functions that aid in survival: humans can use their vision to read and comprehend information discovered centuries ago, navigate across the globe, or even find beauty and meaning in abstract shapes and colors. Vision allows us to act on our motivations while also integrating our environmental demands; overall, this requires that our brains integrate internal and external information and constantly update this information based on changes in the external environment or within ourselves. As a whole, this dissertation is focused on this question: how do our brains allow us to interact in the world?

Described simply, organisms' are able to interact in the world though a basic feedback loop comprised of three main segments: input, processing, and output. At the input stage, organisms acquire sensory information through optimized movements of sensory epithelia, such as through sniffing or movements of eyes, head, or body, for example. Once this sensory information regarding the external world is processed, the brain must integrate this with internal information, such as what is the current state of the animal, or the current motivation or goal. Ultimately, the combination of external and

internal information generates perception. Finally, the brain must use this information to plan an appropriate output or action in order to achieve the desired goal of the organism. This output will then affect the external input acquired, and the feedback cycle repeats. This feedback between input, processing, and output is critical to survival, as the environment is constantly changing, as is the place of organisms within their dynamic environments. The power of this feedback loop is that it allows organisms to make the appropriate changes to their behaviors based on contextual information from both external and internal environments.

This dissertation is comprised of two main projects focused on different segments of the described feedback loop that allows environmental interactions between the world and organisms. In Chapter III, I will describe a projected centered around the input stage. More specifically, this project describes how mice coordinate head and eye movements to optimize gaze stabilization during free movement under a goal-directed context. Chapter II is focused on the processing step of the feedback loop and will describe how external and internal states may be integrated for the generation of accurate sensory perception. In this study, I manipulated a neural substrate known to alter the output of the processing step (i.e., sensory perception). This was achieved using a hallucinogenic compound, DOI (2,5-Dimethoxy-4-iodoamphetamine) which is strongly selective for the serotonin-2A receptor (5-HT_{2A} R).

Mice as a model system for visual processing

The following studies are conducted in one of the leading model systems in the study of mammalian vision, the mouse. Mice are a popular model system for vision for

multiple reasons, but primarily because and it is a model amenable to genetic manipulations for access to specific neuronal populations (Huberman and Niell, 2011), which is incredibly powerful when attempting to dissect neural circuit function. As an added benefit, mice have many similarities to primate brain anatomy and function (Niell and Stryker, 2008; Niell and Stryker, 2010; Huberman and Niell, 2011), meaning that many of the same principles found across decades of vision research in primates can be applied to mouse vision. Even more powerful, however, is that hypotheses about neural circuit function (and development) formed from research in primates can be tested in mice using genetic tools.

Additionally, mice, once considered blind, use their vision to achieve goal-directed tasks in both natural and laboratory settings (Sarko et al., 2011; Huberman and Niell, 2011), though much less is known about mouse vision in the wild. In lab settings, mice use their vision in freely-moving and naturalistic behavioral paradigms in both artificial and ethologically relevant contexts (e.g., Morris water maze, nest building, prey capture; (R. G. M. Morris 1981, Clark, Hamilton, and Whishaw, 2006, Hoy et al., 2016).

Overall, mice are used as a model system for vision because vision mediates some quantifiable behaviors in mice, they have anatomical and functional similarities to primates, and ultimately, because of the powerful genetic tools available in mice.

Serotonergic modulation of visual processing in awake mouse V1

Accurate sensory perception is thought to be generated by the balance of internal and external information processing streams (known as top-down and bottom-up, respectively; Cassidy et al., 2018; Grossberg, 2000). Overweighting of internal representations and/or underweighting of external representations places excessive reliance on prediction at the expense of sensory input, which works to generate hallucinations, or misinterpretations of the external environment (Grossberg, 2000). One such example is in the case of prolonged sensory deprivation, where lack of incoming sensory information is compensated for by overactive internal expectations of what one should experience (Sacks, 2012). Another example of internal/external information imbalance similar to hallucination, is during the state of dreaming. Top-down information (i.e., internal information) is overweighted because there is no incoming external visual information. This imbalance can create incoherent images, thoughts, or emotions which are not always grounded in the material world (Grossberg, 2000).

Hallucination is a positive symptom of some neuropsychiatric disorders, such as Schizophrenia and Bipolar disorder, and is thought to be driven by upregulation of serotonin-2A receptors in the brain (5-HT_{2A} Rs; Muguruza et al., 2013), antagonism of which reduces the frequency of hallucination (Sullivan et al., 2015). Interestingly, activation of 5-HT_{2A} Rs in non-affected individuals by psychedelic drugs such as LSD and psilocybin generates hallucinations, further suggesting a central role of this receptor in mediating changes in sensory perception, hallucinations, and the integration of top-down and bottom-up processing streams. As such, hallucinogenic drugs that selectively

bind to 5-HT$_{2A}$ receptors can be utilized as a tool to understand cognitive, psychophysical, and physiological aspects related to hallucination.

Though the cognitive and psychophysical effects of 5-HT$_{2A}$ R activity have been extensively studied (reviewed in Nichols 2016), the impact of this activation on visual processing remains unknown. Moreover, the connectivity and function of primary visual cortex (V1) make it an advantageous brain region for studying top-down and bottom-up balancing. There have been few studies of individual V1 neuron responses to visual stimuli following administration of 5-HT$_{2A}$R agonists, yielding varying findings of suppression, facilitation, or bidirectional changes in firing rate (Rose and Horn, 1977, Fox and Dray, 1979, Dray et al., 1980, Watakabe et al., 2009). Furthermore, these studies were conducted in anesthetized animals, did not measure individual neuron-tuning properties, or any population-level activity, and did not address cell-type or layer specificity. With recent technological advances in recording population and single-neuron activity in awake animals, we overcame these previous limitations.

For these experiments, we recorded neural activity of individual neurons and populations of single neurons in primary visual cortex (V1) in response to the presentation of visual stimuli before and after pharmacological manipulation of 5-HT$_{2A}$ receptors using the selective 5-HT$_{2A}$ receptor agonist, DOI (2,5-Dimethoxy-4-iodoamphetamine). Different methods were used for neural recordings, each aimed at a particular scale, from whole-brain activity to spiking activity from isolated single units. At the global and population levels, we used *in vivo* calcium imaging using transgenic

mice expressing the fluorescent calcium sensor, GCaMP6s in excitatory cortical neurons. At the global scale, we used widefield calcium imaging, which is advantageous for observing whole-brain activity. Zooming in, at the population level, we used *in vivo* 2-photon calcium imaging to simultaneously record activity of hundreds of neurons in layer 2/3 of V1. Though these two imaging methods afford high spatial resolution (i.e., the experimenter can select any brain region on the dorsal surface of cortex and also view many neurons simultaneously), its temporal resolution is slow, due to acquisition rates and latency and decay of the fluorescent calcium signal which is used as a proxy of neural activity. With these factors together, 2-photon imaging provides information about neural responses within roughly 100 millisecond time bins. To obtain finer temporal resolution (i.e., instantaneous responses of neurons), we recorded the activity of isolated single units across cortical layers in V1 using multi-site silicon probes.

Examination of hallucinations using 5-HT_{2A} activation instead of sensory deprivation or during dreaming is advantageous because there is a specific neural substrate to manipulate. Without a visual stimulus, we would not be able to understand visual contextual modulation because there would be no external visual stimulus and thus, no visually evoked activity.

Serotonergic Hallucinations in Humans

In humans, activation of 5-HT_{2A} receptors drives hallucinations (Butler et al., 1996). Again, this occurs in patients with Schizophrenia, through an upregulation of 5-HT_{2A} receptor expression (Muguruza et al., 2013). Additionally, hallucination occurs in

non-affected individuals following administration of 5-HT$_{2A}$ receptors (Meltzer et al., 2006). Changes on cognition and psychophysics by 5-HT$_{2A}$ activation are beyond the scope of this dissertation, but I will describe their known effects on visual psychophysics and visual information processing specifically in humans.

In the context of visual perception and visual psychophysics following 5-HT$_{2A}$ activation (i.e., in patients with Schizophrenia or after psychedelic drug administration), there are many disparate studies reporting visual perceptual changes, but no unified theory or hypothesis about their overall impact, perhaps because their impact is widespread and highly variable across subjects. Some of these studies report reduced sensitivity to light even 2.3 years after LSD usage (Abraham and Wolf, 1988), reduction in the rate of binocular rivalry switching (Frecska et al., 2004; Carter et al., 2007), changes in only global motion perception, but not local (Carter et al., 2004), increased reaction time during object completion tasks (Kometer et al., 2011), and decreased in object recognition accuracy (Baggott et al., 2010). Within the field, however, some compelling visual psychophysics experiments suggest that the overall visual perceptual dysfunction in Schizophrenia arises from deficits in gain control mechanisms, particularly in computations related to contextual modulation (Butler et al., 2008). For example, patients with schizophrenia have deficits in surround suppression, a type of contextual modulation where a large surrounding stimulus suppresses the neural and perceptual responses to a centrally located target stimulus. In schizophrenia textured patches appear to ‘pop-out’ of background textures due to this deficit (i.e., less surround suppression occurring), whereas they appear more unified to a non-affected individual

(Butler et al., 2008). Chapter II will present some experiments where this is examined at the neural level.

To date, there have been only two studies that have recorded neural activity during hallucinations in patients with Schizophrenia. In the first study, utilizing positron emission tomography (PET), it was observed that patients with Schizophrenia undergo an increase in activity in subcortical nuclei (thalamus and striatum), limbic structures (hippocampus), and paralimbic regions (parahippocampal and cingulate gyri, as well as orbitofrontal cortex). Additionally, they found increased cortical activity in brain regions related to the content of hallucinations (e.g., inferotemporal cortex activation during hallucination of facial structures; Silbersweig et al.,1995). Using fMRI, the second study, conducted by Oertel and colleagues (2007), found increased activity related to hallucinations in higher-order cortical visual areas related to processing complex visual stimuli such as faces, bodies, and scenes. Intriguingly, activation of these areas coincided with the content of the subject's hallucinations. In addition to increased activity in higher order visual areas, the experiments also discovered increased hippocampal activity during visual hallucinations, which they posit is derived from the retrieval of visual images from memory. Neither of the studies reported significant increases in activation of early visual areas or prefrontal cortices.

These two studies had slightly conflicting results (the second study did not note any changes in subcortical activity, besides in hippocampus), potentially due to the medication status of the patients, as the first study combined medicated and unmedicated

patients and the second study was from one medicated patient only. The medicated patients across both studies also took different medications at different doses. To date, systematic studies of hallucinations in patients with Schizophrenia have not been conducted thoroughly. As such, the use of psychedelic hallucinogens that activate 5-HT_{2A} receptors have been popularized as a tool to study the neural mechanisms driving the generation of hallucinations and for the treatment of mental health disorders (Johnson and Griffiths, 2017; Carhart-Harris and Goodwin, 2017).

In a groundbreaking and provocative study, Carhart-Harris et al. (2012), found a strong reduction in BOLD signal in anterior and posterior cingulate cortices and thalamus, as well as a decrease in functional connectivity across brain networks (a measure of how correlated, and functionally related disparate brain regions are in their activity). Up to this point, a decrease in brain activity related to hallucinogens had not been observed because a truly systematic study had not been conducted. This study opened a new avenue of research on the activity of hallucinogens in the human brain, a topic that has interested humans since prehistoric times (Guerra-Doce, 2015).

Most studies hallucinogenic 5-HT_{2A} receptor activation in humans, however, are not concerned with visual processing or visually evoked activity. The few studies that investigate visually evoked activity focus on abnormal oscillatory brain activity, as patients with schizophrenia have large decreases in LFP power at both alpha and gamma frequency bands in multiple brain regions (Green et al., 1999; Williams & Boksa, 2010). This abnormal oscillatory brain activity is used as a biomarker for schizophrenia (Moran

& Hong, 2011). Similarly, alpha and gamma power decreases are observed in human imaging studies following $5HT_{2A}$ agonist administration (Kometer, et al., 2015; Nichols, 2016). Oscillations mediate rhythmic cortical inhibition and it is proposed that this effectively shifts the resting excitation/inhibition balance (Kometer et al., 2013; Kometer et al., 2015). This is expected to disrupt the ordinary temporal structure of neuronal processes, though this is not yet understood at a cellular or neural population level, which is one of the motivations driving the project described in Chapter II, where I provide the first evidence that this was indeed the case at the level of small populations of individual neurons in V1, both at the level of LFP activity and single-unit spiking (Michaiel et al., 2019).

But where do hallucinations arise? Previously, the most prevalent model, thalamic filter model, predicted that hallucinations were generated in the thalamus. This model posits that limbic cortico-striatal-thalamic-cortical feedback loops (CSTC) function to prevent excessive exteroreceptive information flow to cortex as well as to prevent internal overexcitation (Carlsson and Carlsson, 1990). It was hypothesized that in Schizophrenia and with serotonergic hallucinations in general, sensory gating between thalamus and cortex is disrupted, leading to excessive sensory input to the cortex, consistent with behavioral reports of psychosis Vollenweider, 2001; Vollenweider & Geyer, 2001). Recent studies have suggested that hallucinogenic $5HT_{2A}$ agonists, however, do not require activation of presynaptic $5HT_{2A}$ receptors in thalamocortical afferents (Puig et al., 2003; Gonzalez-Maeso et al., 2007). In a series of ground-breaking experiments, Gonzalez-Maeso et al. (2007) utilized transgenic mice that only expressed

5HT$_{2A}$ receptors in cortex, and no subcortical regions. Upon pharmacological activation of 5HT$_{2A}$ receptors *in vivo,* mice still displayed behavior consistent with readouts of hallucination in mice (for example, the head twitch response), suggesting that 5HT$_{2A}$ expression in thalamus, or any subcortical region, is not required for hallucination. Instead, disrupted feedback modulation may arise from cortico-thalamic projections (rather than thalamo-cortical), specifically from layer V, which functions as an output layer of the cortex (Sapienza et al., 1981). 5HT$_{2A}$ is also most highly expressed in layer V pyramidal neurons (Lopez-Gimenez et al., 2001). These projections are thought to engage in sensory gating functions to modulate cortical-subcortical communication. This point is one of the motivators for electrophysiological recordings in layer 5 neurons, described in detail in Chapter II.

As seen from the research reviewed above, much of the research and findings of 5HT$_{2A}$ activity, whether in patients with Schizophrenia, or following psychedelic drug administration, is variable. Due to government regulation of 5HT$_{2A}$ agonists like LSD, progress in this field has been slower than other areas in neuroscience. The experiments in Chapter II aimed to unify hypotheses in the field while also providing the first neurophysiological studies of 5HT$_{2A}$ activity in visual brain areas *in vivo*.

Expression of 5-HT$_{2A}$ receptors in the mammalian brain

Within the brain, 5-HT$_{2A}$ is expressed postsynaptically to serotonergic neurons, in both cortical and subcortical structures. Subcortically, in subcortical structures, it is highly expressed in the basal ganglia, claustrum, and limbic areas (amygdala and

hippocampus) (Hensler 2012). Within the mammalian cortex, it is most densely expressed in the prefrontal cortex, but out of all of the primary sensory areas, 5-HT_{2A} receptors are expressed most densely in primary visual cortex (V1) (Hensper, 2012). Interestingly, this receptor is expressed in both glutamatergic excitatory projection neurons and local GABAergic inhibitory neurons (Celada et al., 2004). Additionally, 5-HT_{2A} receptors are differentially expressed in different cell types within excitatory/inhibitory neuron classes, making its function difficult to define (Weber and Andrade, 2010).

Visual cortex, like other primary cortical areas, is organized in six layers, each defined by their function and cytoarchitecture (Larkum et al., 2018). Each of these layers derives its function from its composition of cell-types and connectivity to other cells/and or layers (Larkum et al., 2018). Within V1, 5-HT_{2A} is expressed across all cortical layers, but most densely in layer 5 neurons, then layer 2/3 (Weber and Andrade, 2010). I will discuss layer and cell-type specificity of serotonergic modulation on visual processing in V1 in detail in Chapter II.

From these experiments, at a range of different levels of analysis, we found dramatic reductions in response gain and surround suppression (a form of contextual modulation related to external visual features) and altered temporal dynamics but no changes in basic tuning properties. These results, described in detail in Chapter II, suggest an imbalance between internal and external processing streams, with an overall reduction in sensory drive, or underweighting of information related to external features.

This may ultimately lead to misinterpretation of the visual world, due to lack of sensory evidence and/or overweighting of internal information (such as expectation built on prior information) consistent with current models of hallucination.

Classes of Eye Movements: saccades, smooth pursuits, and fixational eye movements

Vision is an active process (Rucci and Poletti, 2014; Otero-Millan et al., 2008). Organisms move their eyes through the world to acquire particular types of information based on the current goal (Yarbus, 1976). These movements, broadly classified into three types, saccades, smooth pursuits, and fixational eye movements, are optimized for active visual sampling across the visual world (Gegenfurtner 2016).

Though there are multiple types of saccadic eye movements, characterized by the speed and amplitude at which they occur, overall saccades are defined as rapid eye movements that voluntarily or involuntarily shift the center of gaze to a new target visual location. These types of eye movements were initially illustrated by a vestibular researcher, Crum Brown, who noticed these rapid eye movements did not compensate for movements of the head. It was not until French ophthalmologist, Émile Javal, used the word ‘saccade’ (French for ‘jerk’) to describe these rapid non-compensatory eye movements that they became a popular topic for research (Wade, 2010).

Smooth pursuit movements, like saccades, also voluntarily or involuntarily shift the position of gaze to a new target, but do so more gradually (Ono and Mustari, 2008). Smooth pursuit movements allow primates, birds, and foveate animals to track moving objects (Fukushima et al., 2013) by maintaining the visual target on the fovea.

Mechanisms driving smooth pursuit movements in non-foveate animals, like mice, are poorly understood, but these movements can be evoked by slow moving visual stimuli when the animals are restrained (Mitchiner et al, 1975). Interestingly, however, smooth pursuit movements in rodents are typically thought of as reflexive and stabilizing for motion occurring in the external world. For example, during free movement in rodents, stabilization of moving visual stimuli occurs through the optomotor response (i.e., compensatory head movements). In contrast, during head fixation, stabilization for moving visual stimuli occurs instead through compensatory eye movements mediated through the optokinetic response (Kretschmer et al., 2017). Currently is no evidence of voluntary smooth pursuit movements in rodents like those seen in foveate animals.

Finally, fixational eye movements are slight, imperceptible movements in eye position during fixation, when the gaze is stabilized, or fixed, over a single point. There are three main classes of fixational eye movements: microsaccades, ocular drift, and tremors, each defined by their speed, amplitude, and frequency (reviewed in Rucci and Poletti, 2014) and their modulation by external and internal factors (e.g., illumination conditions and attention, respectively; reviewed in Martinez-Conde et al., 2004). The function of fixational eye movements is unknown, though they are proposed to either prevent neural adaptation from prolonged exposure to a visual stimulus or enhance visual sampling by exposing different areas of the retina to the visual image (Martinez-Conde et al., 2004).

Together, saccades, smooth pursuits, and fixational eye movements are all utilized to optimize visual sampling under goal-directed contexts (Gegenfurtner 2016). Traditionally, these eye movements have been studied in foveate animals, potentially due to technical hurdles in recording these movements in freely behaving animals or because non-foveate animals do not display some of these types of eye movements. As such, Chapter III of this dissertation is focused on investigating some of these eye movements (particularly saccades) in a non-foveate animal, the mouse. Chapter III will not discuss fixational eye movements because their amplitude is small (~1 degree; Martinez-Conde et al., 2004), and would require more a more temporally and spatially precise recording technique than ocular videography to achieve reliable results. Smooth pursuit movements in non-foveate animals take the form of compensatory head movements achieved through the ocular motor reflex (Kretschmer et al., 2017). Ongoing work related to Chapter III is focused on determining if there are any smooth pursuit eye movements that are not reflexive, and hence, more similar to smooth pursuit eye movements observed in foveate species.

Visual Predation & Binocular Vision in Rodents

The visual predation hypothesis, proposed by evolutionary biologist Matt Cartmill (1974), states that primates evolved in response to preying on insects and other small creatures. Over time, in practice this meant that primates evolved foveate and binocular vision in order to capture centrally located prey. Though this visual predation hypothesis is compelling in the context of the evolution of primate vision, it disregards predators outside of the primate order. As such, the visual predation hypothesis has been expanded

to describe general features of eye placement and visual capabilities of prey and predators (Cartmill, 1992).

Typically, predators, such as humans and non-human primates, have front-facing eyes which creates wide binocular fields, allowing for depth perception and effective hunting (Cartmill, 1974). This wide binocular field is generated because there is a large overlap of the monocular areas (i.e., the view that each eye sees individually) because the eyes are close together. This was first explained by the Egyptian scientist Ibn al-Haythum (known as the father of modern optics) in his book Kitab al-Manazir (translated to 'Book of Optics') which was written between 1011 and 1021. In contrast to predators which have front facing eyes, prey typically have lateral facing eyes, and thus large monocular fields and an overall wide field of view, which allows reliable motion detection of approaching predators in the periphery (Cartmill, 1974). In humans, the binocular area, the area of fusion between the view of the two eyes, is roughly 135 degrees, as opposed to 40 degrees in mice (Heesy, 2004). Overall, prey have wide monocular areas at the expense of wide binocular vision, and the opposite is generally true of predators.

However, predator and prey classifications are not always accurate, as many animals can act as both predators and prey depending on the context. This is clear when considering food chain interactions within an environment, which was first described by the Arab Scholar, Al-Jahiz, in the 7th Century in the book Kitab-al-Haywanat (Book of Animals). Similar to many other scientific ideas first described in Medieval Arabia, this concept was popularized and re-described by Western imperialists following the

popularization of natural selection theories (Zirkle, 1941). Mice, generally thought of as prey animals, can act like predators, even though they have these characteristics of prey. For example, mice are prey to snakes and birds, while also being predator to insects.

Modulation of V1 activity by locomotion

As mentioned previously, a prevalent topic of exploration in the context of vision is modulation of visual processing by locomotor signals, which was first described in detail by Niell & Stryker (2010). More specifically, locomotion has been found to increase the gain of neural responses in V1, while maintaining selectivity and tuning properties, ultimately increasing the signal to noise ratio for visual information in the brain. In mice, locomotion co-varies with arousal, attention, and reward. As one would predict, increasing the gain of visual responses during locomotion, then aids in encoding of sensory representations (Dadarlat and Stryker, 2017) and resulting visual learning and behavior.

The presence or absence of locomotion in an awake animal has become associated with behavioral state, though very little is known about what locomotor signals in sensory areas mean for the brain. The next topic of my dissertation lays the groundwork for these queries: what does self-motion mean to the brain, particularly in the context of sensory systems? How is locomotion driven by incoming sensory evidence? How does locomotion help animals achieve goals that require rapidly changing sensory information? Together, these questions encompass the most prevalent question in sensory systems neuroscience: How do animals acquire sensory information and use it to drive behavior?

Current limitations in head-fixed visual neurophysiology

Due to previous technical constraints, most studies examining the modulation of V1 activity by locomotion are head-fixed such that animals are not actually moving through the environment, or receiving appropriate visual flow-field signals, nor are normal vestibular signals being integrated in V1 activity. Recent efforts to implement virtual reality paradigms and stimulus conditions aim to eliminate this confound by providing a virtual but controlled environment for animals to explore and perform visually guided tasks (Saleem et al., 2018). Though virtual reality paradigms produce more realistic visual flow-field stimuli, they do not fully recapitulate natural motion because the animals are unable to move their heads in three dimensions like they would typically do. As such, normal vestibular signals from self-motion are not present. Additionally, gaze position is known to be a powerful modulator of V1 activity and tuning features position (Weyand and Malpeli, 1993; A. P. Morris and Krekelberg, 2019), though this is not studied in mice because rodents rarely move their eyes while headfixed (Wallace et al. 2013; Payne & Raymond, 2017), even in virtual reality contexts.

As stated, most studies of visual processing are conducted under conditions of head- and gaze-fixation in order to control visual input to the retina, and thus, make conclusions about neural representations of visual features. While these studies have been essential in understanding visual processing under stationary viewing conditions, head- and gaze-fixation severely limit organisms' natural exploration of the world, which is naturally accomplished through directed head, body, and eye-movements (Yarbus, 1976).

Unlike several other subfields within neuroscience, visual neurophysiology has not yet adopted freely-moving paradigms. Primarily this is because to understand visual representations, one must know the visual input to the system i.e., what the organism is seeing. To move towards a more comprehensive understanding of visual processing and its modulation by movement (head, body, and eyes), freely moving paradigms should be adopted.

Prey capture as a visually guided and ethologically relevant behavior

Capture of live cricket prey by mice is a visually guided and ethologically relevant behavior (Hoy et al. 2016). In the absence of visual cues (i.e., in darkness), mice cannot reliably capture crickets, unless the cricket is within reach of the mouse, where likely other sensory cues are engaged (primarily auditory or tactile cues from whiskers). It is an open question as to what behavioral sampling and oculomotor strategies mice may use to successfully achieve this behavior. Mice, like most prey animals, are primarily monocular animals due to the lateral placement of the eyes on the head. The small monocular overlap creates a narrow binocular field of roughly 40 degrees (as opposed to roughly 135 degrees in humans; Heesy, 2004). Mice are also not foveate animals, meaning they do not have a concentrated section of the retina with densely packed photoreceptors where high acuity vision is localized. Commonly studied eye movements, such as smooth pursuit movements, are believed to be utilized for stabilization of important visual targets on the fovea (Ono and Mustari, 2008), but less is understood about active eye movements during motion in non-foveate animals. This suggests that mice may use a strategy different from foveate or primarily binocular animals to maintain visual targets in front of them while locomoting.

As a whole, little is known about eye movements during goal-directed visual behaviors in afoveate animals. How do animals with no fovea and primarily monocular vision regulate their gaze to track visual targets? The animal kingdom has evolved several strategies to solve this problem. One of these strategies, known as binocular fixation (seen in chameleons and starlings), occurs in both foveate and non-foveate animals with laterally facing eyes, and consists of converging both eyes nasally to create an area of monocular overlap in front of the head (Schwab, 2001). Another strategy (utilized by chickens and some other avian species), in contrast, is to move the head in order to shift gaze onto the target location (Dawkins, 2002). Interestingly, some birds with laterally-facing eyes increase the frequency of their head movements while engaged in goal-directed visual tasks (Dawkins, 2002).

To understand how afoveate and primarily monocular animals track visual objects, I have designed a system to binocularly record eye movements while an overhead camera records head and cricket position while mice perform prey capture behavior. The results of these experiments are presented in detail in Chapter III. In summary, I have found that mice use a strategy in which they bilaterally center their eye position, and make a combination of saccade-like readjustments of eye position and compensatory eye movements to stabilize prey in the binocular zone.

These studies will lay the foundation for future studies of visual processing in naturally behaving animals and will yield a more realistic understanding of visual feature

encoding. For example, gaze position is known to modulate features encoded by neurons in V1, such as receptive field size, and this paradigm allows for free movement of gaze. This method can be easily adapted to include neural recordings. With a slight modification of the described paradigm it will be possible to bypass the need for headfixation to understand the process of vision. Instead of two eye-facing cameras, one of them could be pointed outwards towards the world to record the perspective of the mouse during free movement. Using the recorded visual scene and the movement of the eye, one could calculate the visual stimulus and observe behavior or neural activity driven by the computed stimulus. I have conducted these experiments and the analyses are ongoing. Overall, this new experimental paradigm will allow for a more realistic study of contextual modulation of visual processing.

CHAPTER II

A HALLUCINOGENIC SEROTONIN-2A RECEPTOR AGONIST REDUCES VISUAL RESPONSE GAIN AND ALTERS TEMPORAL DYNAMICS IN MOUSE V1

JOURNAL STYLE INFORMATION

Angie M. Michaiel*, Philip R.L. Parker*, Cristopher M. Niell. Reproduced in part from *Cell Reports*, 2019. Copyright 2019.

*Authors contributed equally

AUTHOR CONTRIBUTIONS

A.M.M., P.R.L.P, and C.M.N. conceived of the project, designed experiments, analyzed data, and wrote the manuscript. A.M.M. performed electrophysiology experiments, P.R.L.P. performed two-photon imaging experiments, and A.M.M. and P.R.L.P. equally performed widefield imaging experiments.

INTRODUCTION

Both externally (bottom-up) and internally (top-down) driven representations of the world contribute to sensory perception. Disruption of accurate sensory perception, as occurs during hallucination, is hypothesized to result from increased top-down and/or decreased bottom-up signaling, leading to excessive reliance on prediction at the expense of sensory input (Cassidy et al., 2018, Grossberg 2000). Abnormal serotonin-2A receptor (5-HT_{2A}R) activity is implicated in sensory hallucination, defined as the misinterpretation of sensory stimuli in space or time or the perception of an absent external stimulus. In

particular, hallucinations and altered perception resulting from both schizophrenia and psychedelic drug administration are prevented by antagonism of 5-HT$_{2A}$Rs, supporting a central role of this receptor in mediating hallucinations (Schmidt et al., 1995, Vollenweider et al., 1998).

The cognitive and perceptual effects of 5-HT$_{2A}$R modulation have been extensively studied, particularly in the context of psychedelic drugs (reviewed in Nichols, 2016). Recent studies have begun to elucidate the action of serotonergic hallucinogens on large-scale brain activity in humans using neuroimaging methods (Preller et al., 2018, Carhart-Harris et al., 2016). However, the impact on sensory information processing at the level of single neurons and populations of neurons is largely unknown. To our knowledge, measures of visually evoked responses after 5-HT$_{2A}$R agonist administration in humans are limited to one study, which showed large reductions in pre-stimulus alpha-band LFP synchronization (Kometer et al., 2013). There have been few studies of individual V1 neuron responses to visual stimuli following administration of 5-HT$_{2A}$R agonists, yielding varying findings of suppression, facilitation, or bidirectional changes in firing rate (Rose and Horn, 1977, Fox and Dray, 1979, Dray et al., 1980, Watakabe et al., 2009). Furthermore, these studies were conducted in anesthetized animals, did not measure individual neuron-tuning properties, and did not address cell type or layer specificity.

The selective 5-HT$_{2A}$R agonist DOI (2,5-dimethoxy-4-iodoamphetamine) is known to be a powerful hallucinogen in humans (Shulgin and Shulgin, 1991) and has been used

extensively to study 5-HT$_{2A}$R function in animal models, particularly of schizophrenia and psychedelic drug action (for reviews, see Hanks and González-Maeso, 2013, Nichols, 2016). In this study, we assessed the impact of DOI on visual processing at multiple scales, from retinotopic maps to individual neurons, using widefield and two-photon calcium imaging and single-unit electrophysiology in awake, head-fixed mice. Our results demonstrating how a serotonergic hallucinogen disrupts sensory processing should provide a deeper understanding of how cortical circuits generate a representation of the world based on sensory input.

MATERIALS AND METHODS

Experimental Model and Subject Details

All procedures were conducted in accordance with the guidelines of the National Institutes of Health and were approved by the University of Oregon Institutional Animal Care and Use Committee. Two- to eight-month old adult mice [C57BL/6J for electrophysiology, CaMKII-tTA:tetO-GCaMP6s (Jackson Laboratories stock numbers 007004 and 024742) for imaging (Mayford et al., 1996, Wekselblatt et al., 2016)] were initially implanted with a steel headplate over primary visual cortex to allow for head-fixation during electrophysiology (Niell and Stryker, 2008) or imaging (Wekselblatt et al., 2016) experiments. In total, 26 male and 39 female mice were used for this study. Animals were handled by the experimenter for several days before surgical procedures, and subsequently habituated to the spherical treadmill for several days before experiments. Some mice in imaging experiments were previously trained on a two-alternative forced choice task, where they were water restricted and given water rewards based on leftward or rightward movements of the spherical treadmill during luminance

discrimination and orientation/spatial discrimination of a grating patch (for details, see Wekselblatt et al., 2016). The grating patches presented during passive viewing in this study were similar in quality (45 deg, 0.16 cycles/degree for behavior, see below for passive parameters) but presented in a different location in visual space compared to the previous behavioral training. These mice were not water restricted during the current experiments, and imaging experiments performed under identical conditions as naive groups.

Surgical procedures

Animals were anesthetized with isoflurane (3% induction, 1.5%–2% maintenance, in O_2) and body temperature was maintained at 37.5°C using a feedback-controlled heating pad. Fascia was cleared from the surface of the skull following scalp incision and a custom steel headplate containing a circular well was attached to the skull using Vetbond (3M) and dental acrylic. The headplate well was centered over V1 (2.5-3 mm lateral of the midline and 1 mm anterior of Lambda). Carprofen (10 mg/kg) and lactated Ringer's solution were administered subcutaneously, and animals were monitored for three days following surgery.

For widefield imaging, a protective layer of cyanoacrylate adhesive (Loctite) was applied to the skull within the headplate well (10 mm diameter) during headplate attachment. For two-photon experiments, a second surgery was performed at least 3 days after headplate attachment, whereby a section of skull ~5 mm in diameter was removed via dental drill, artificial dura (Dow-Corning 3-4680 Silicone Gel) was applied in the craniotomy, and a 5

mm glass coverslip was glued into place over the craniotomy. Antibiotics (cefazolin, 10 mg/kg) were administered in the week surrounding the surgery, and an anti-inflammatory (dexamethasone, 10 mg/kg) was administered 18h and 2h prior to surgery to prevent brain swelling.

For electrophysiology experiments, at least two days following headplate attachment a craniotomy (1 mm diameter) was made the night before or several hours prior to the recording session. The cortical surface was covered with a layer of 1.5% agarose in 0.9% saline and a layer of Kwik-Sil (WPI) to prevent drying and provide structural support.

Experiments

Mice were head-fixed above a spherical treadmill and locomotion was measured via an optical mouse placed on the side of the spherical treadmill using a custom MATLAB script. Visual stimuli were generated in MATLAB using the Psychophysics toolbox extensions (Brainard, 1997, Pelli, 1997), and presented on gamma-corrected LED monitors oriented tangentially 20-25 cm from the contralateral eye (plus ipsilateral eye for widefield retinotopic mapping). Saline (0.9% NaCl) or DOI (Sigma, 10 mg/kg in saline) was then administered subcutaneously, and visual responses to the same stimulus set (presented in reverse order) were recorded again after a waiting period of 15-20 min. Mice were monitored for front paw stereotypy, which DOI reliably induced within 5-7 min following injection.

This dose of 10 mg/kg was chosen based on standards in the literature, which range from 1-10 mg/kg intraperitoneal (Freo et al., 1992; Aulakh et al., 1992; Garcia et al., 2007; González-Maeso et al., 2007). Subcutaneous injection was used rather than intraperitoneal to prevent having to remove the animal from the head-fixed setup between pre and post stimulus presentations. We estimate that our effective dose is approximately equivalent to 2.5 mg/kg intraperitoneal based on previous comparisons of the two injection methods, where serum levels tend to rise more slowly and peak at significantly lower concentrations after subcutaneous injection (Porter et al., 1985, Turner et al., 2011, Turner et al., 2011, Hirota and Shimizu, 2012). Previous work revealed LSD elicited head bob behavior in rabbits occurs independent of the route of administration (Schindler et al., 2012). However, to confirm that we were not using an excessively high dose, we tested a lower dose in a subset of widefield experiments (2 mg/kg subcutaneous) and saw no significant change in response amplitude relative to baseline (see Figure S1).

Widefield Imaging

A widefield microscope (Scimedia, Inc.) equipped with a sCMOS camera (PCO, 10 Hz acquisition) was used to measure GCaMP6s signal though the skull during blue LED excitation (Luxeon Rebel 470 nm, 0.1 mW/mm^2 at the sample). In a subset of experiments, a green LED (Luxeon Rebel 530 nm, 0.1 mW/mm^2 at the sample) was used for excitation every four frames to measure hemodynamic signals, which were subtracted from the blue frames (Wekselblatt et al., 2016). The change in fluorescence relative to baseline ($\Delta F/F$) was calculated for each pixel individually using its mean value as F. Visual areas were first mapped using a topographic stimulus consisting of a bar of 1/f noise sweeping in either azimuth or elevation, and the amplitude and phase of the Fourier

component of the ΔF/F signal were calculated at the stimulus frequency (0.1 Hz), which were later used to align sessions across animals (Kalatsky and Stryker, 2003). Vertical and horizontal stationary grating patches (0.16 cpd, 30 deg) were presented to the right eye with 1 s duration and 1 s inter-stimulus interval. For each animal, a central point in V1 corresponding to the approximate response peak was selected, and the pixels around this point in a 5 X 5 region were averaged to create ΔF/F traces. To analyze spatial spread of responses, an elliptical meshgrid was generated around this central point, with a 2:1 ratio of the major:minor axes aligned in the anteroposterior:mediolateral dimensions to account for cortical magnification factor, and the points along this meshgrid radiating out from the center were averaged along these concentric ellipses to create an average ΔF/F for a given distance from the center point along the minor axis of the ellipse. Normalized ΔF/F change was calculated as (post-pre)/mean(post,pre).

Two-photon imaging

A two-photon microscope (Neurolabware, 16X Nikon CFI75 LWD objective) was used to measure GCaMP6s signal through the cranial window at 920 nm laser excitation (Mai-Tai, Spectra-Physics). ~800 μm by 800 μm frames were acquired at 10 Hz using Scanbox software. Visual areas were first mapped using widefield imaging (described above), then V1 was targeted and the stimulus screen and field of view were adjusted to center the visual response. A mapping stimulus (see widefield imaging methods) was first used to measure spatial receptive fields, followed by a period of darkness (5 min) to measure spontaneous activity. Then a ~22 min stimulus was shown to measure surround suppression, which consisted of binarized grating patches at various sizes (5, 10, 20, 30,

40, and 50 deg of visual field), spatial frequencies (0.04, 0.16 cycles/deg), and orientations (0, 90°) at a 2 Hz temporal frequency and full contrast, with 0.5 s duration and 0.5 s inter-stimulus interval.

Cell footprints were extracted using constrained nonnegative matrix factorization, with a spatially homogeneous neuropil response factored out (Pnevmatikakis et al., 2016). ΔF/F was calculated for all pixels using the 10th percentile as F, and then traces for all cells were deconvolved using constrained foopsi. Data for each specific stimulus were then analyzed using custom MATLAB scripts. For surround suppression data, ΔF/F within each inter-trial-interval was averaged and subtracted from the ensuing trial, and the ΔF/F traces during blank stimuli (mean luminance gray identical to inter-trial-interval) were averaged across the experiment and subtracted from all trials (separately for stationary and running trials). Only neurons whose somata were within the region of neuropil activated by the 10 deg stimulus were included in the analysis, constrained within an elliptical region with a 2:1 major:minor axis ratio along the anteroposterior:mediolateral dimensions to account for cortical magnification factor, with a manual rotational offset and overall size chosen to closely match each individual animal's response pattern. Within this region, only neurons with responses to any one of the stimulus types (combination of size, spatial frequency, orientation) greater than 10% ΔF/F for both pre and post drug injection were included in analyses. For all two-photon group analyses, averages were taken across cells (within animal) and these values were then used to calculate group mean/standard error. For surround suppression experiments, a divisive normalization model (

Ayaz et al., 2013) was used to fit the data for pre and post injection periods separately, then all variables except R_D and R_S were constrained as the average of pre/post values, and the fits were run again. The equation fit to each animal's size tuning curve was: where R_D and R_S are the strengths of the driving and suppressive fields, σ_D and σ_S are the extents of the driving and suppressive fields, m is an exponent, d is the diameter of the stimulus, and erf is the error function. The coefficient of determination for each group was: saline naive $r_2 = 0.939$, saline trained $r_2 = 0.928$, DOI naive $r_2 = 0.867$, DOI trained $r_2 = 0.941$, and there was no significant difference between pre and post fit r_2 for any group (paired t test). Suppression index was calculated as $(R_{MAX} - R_{50d})/(R_{MAX} + R_{50d})$ where R_{MAX} is the largest response across all sizes, and R_{50d} is the response to the largest stimulus (50 deg). Normalized change for R_D, R_S, and suppression index was calculated as (post-pre)/mean(post,pre).

Extracellular Multichannel Electrophysiology

Multisite silicon probes (NeuroNexus, A2x32-5mm25-200-177) coated with a small amount of the lipophilic dye DiO (Invitrogen) were inserted through the overlaying agarose and into monocular V1 using a microdrive (Siskiyou Designs). Electrode penetrations were done over the course of 30 min – 1 h and the probe was allowed to settle in its final position for at least 30 min before data collection began. Hand-mapped receptive fields were used to approximately center the screen position on receptive field centers. Contrast-modulated noise movies (Gaussian 1/f) were presented and spike-triggered averaging (STA) was utilized to estimate spatial receptive fields as in Niell and Stryker (2008). Full-field drifting sinusoidal gratings were presented at twelve evenly spaced directions of motion, six spatial frequencies (0.01, 0.02, 0.04, 0.08, 0.16, and 0.32

cpd), and full-field flicker (0 cpd) with temporal frequency of 2 Hz. Stimulus presentations were randomly interleaved for 1.5 s duration, with 1 s inter-stimulus interval. To estimate spontaneous firing rate, a gray blank condition (mean luminance) was also presented. For darkness recordings, the computer monitor was turned off and other sources of light in the room were covered.

At the end of the experiment, animals were euthanized by deep anesthesia and cervical dislocation. Following removal, brains were immersed in 4% PFA (Electron Microscopy Sciences) in PBS at 4°C. 100 μm coronal sections were cut with a vibratome and mounted using Vectashield with DAPI (Vector Laboratories) then imaged on a Zeiss Axio Imager 2 to determine the depth of electrode penetrations. Each site along the electrode was given a layer assignment based on its position on the probe relative to the depth of the probe tip and geometry of the penetration angle. In addition to histology, current source density was also used to identify cortical layers in neural recordings (Hoy and Niell, 2015). Data acquisition was performed as described by Niell and Stryker (2008). Signals were acquired using a System 3 workstation (Tucker-Davis Technologies) and analyzed with custom software in MATLAB (MathWorks). Extracellular signals were filtered from 0.7 to 7 kHz and sampled at 25 kHz. We detected spiking events on-line by voltage threshold crossing, and a 1 ms waveform sample on four adjacent recording sites was acquired, creating a virtual tetrode. Single-unit clustering and spike waveform analyses were performed using a combination of custom software in MATLAB and Klusta-Kwik (Harris et al., 2000), as described previously (Niell and Stryker, 2008). Quality of unit separation was based on a clear refractory

period of less than 0.01% of spikes within a 1 ms inter-spike interval and by the computed *L* ratio (Schmitzer-Torbert et al., 2005). Units were also checked for stability by confirming that their peak amplitude remained consistent over the course of the recording session. Units that were found by histology to be outside of V1 were excluded from subsequent analysis.

Movement signals from the optical mouse were acquired at up to 300 Hz and integrated at 100 ms intervals (Mx310; Logitech), as originally described by Niell and Stryker (2010). By using these measurements, we calculated animals' mean speed for every stimulus presentation. Trials with mean speed above 0.5 cm/s were considered movement trials.

For LFP analysis, the extracellular signal was filtered from 1 to 300 Hz and sampled at 1.5 kHz. The power spectrum was computed using multi-taper estimation in MATLAB with the Chronux package (Mitra and Pesaran, 1999, Mitra and Bokil, 2007), with a sliding window and three to five tapers. Spectra were normalized for presentation by applying a 1/f correction (Sirota et al., 2008). Traces of individual experiments were normalized to the range of either the pre or post recording block across all experiments before averaging.

Units were classified as narrow or broad spiking based on properties of their average waveforms at the electrode site with largest amplitude. As detailed in Niell and Stryker (2008), two parameters—(1) height of the positive peak relative to the initial negative

trough and (2) time from the minimum of the initial trough to maximum of the following peak—were sufficient to generate two linearly separable clusters corresponding to narrow spiking (putative inhibitory) and broad-spiking (putative excitatory) neurons. These clusters were separated using K-means.

Average evoked firing rate was calculated following a baseline subtraction of the spontaneous rate during 1 s inter-stimulus intervals. Modulation indices were calculated for evoked (1 Hz threshold) and spontaneous (0.5 Hz threshold) rates where MI = $(R_{post}-R_{pre})/(R_{post}+R_{pre})$. Peri-stimulus time histograms were calculated using 100 ms time bins over the 1.5 s duration of each stimulus presentation and 1 s ISI. Visually responsive units included in the analysis were defined as units with an average firing rate above 2 spikes/s after baseline subtraction for either pre or post recording blocks.

We calculated preferred angle of orientation by finding the stimulus orientation that elicited the peak response for each cell on average, regardless of spatial frequency. The OSI was calculated as the depth of modulation from the preferred orientation to its orthogonal orientation $\theta_{ortho} = \theta_{pref} + \pi/2$, as $(R_{pref} - R_{ortho})/(R_{pref} + R_{ortho})$. Preferred spatial frequency was determined by finding the spatial frequency that elicited the largest response, on average. We used STAs of individual units recorded before and after drug administration to calculate 2-D correlation coefficients as a measure of similarity of receptive field structure.

Quantification and Statistical Analysis

Two-tailed paired t tests or Wilcoxon Rank sum tests were used to compare data before versus after drug administration. For comparisons between saline and DOI, two-sample

tests such as Kolmogorov-Smirnov or two-sample two-tailed t tests were used. For comparison of trained and naive saline and DOI groups, Kruskal-Wallis and post hoc Tukey-Kramer tests were used. Significance was defined as $p < 0.05$, and in the case of multiple comparisons a Bonferroni correction was implemented.

RESULTS

DOI Reduces Visually Evoked Responses in Visual Cortex

To measure the effects of 5-HT$_{2A}$R activation on spatial and temporal processing in visual cortex, we measured visual responses in mice head-fixed on a spherical treadmill (Dombeck et al., 2007) using widefield imaging and two-photon calcium imaging, and single-unit electrophysiology with silicon probes (Figure 1A). Following presentation of a set of visual stimuli, mice received a subcutaneous injection of either saline (control) or the 5-HT$_{2A}$R agonist DOI (10 mg/kg; see Methods and Figure S1 for an explanation of dose choice), and after a 15- to 20-min waiting period, the stimulus set was repeated. To explore how previous experience with visual stimuli may influence effects of 5-HT$_{2A}$R signaling, we performed a subset of these passive viewing experiments with animals previously trained on a visually guided task, in addition to standard non-trained animals. As visual responses and surround suppression are modulated by behavioral state (Niell and Stryker, 2010, Ayaz et al., 2013), we separated data into stationary or running periods for statistical comparison. Notably, neither pupil size nor fraction of time running was different following drug administration (Figure S2), suggesting that changes observed were not due to differences in behavioral state.

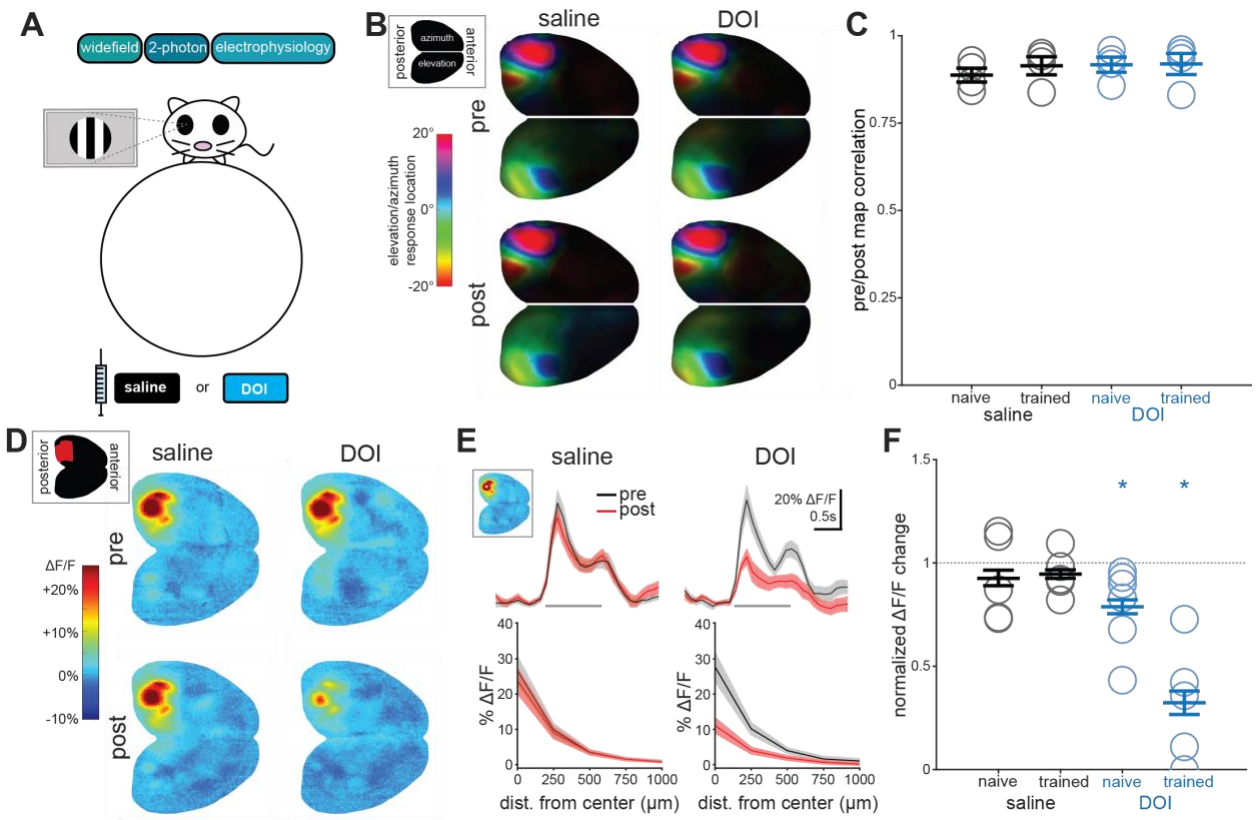

Figure 1. DOI Reduces Visually Evoked Responses in Visual Cortex.

(A) In all experiments, we measured responses to visual stimuli before and 20 min after drug administration using widefield and two-photon GCaMP6s imaging or silicon probe electrophysiology in awake, head-fixed mice on a spherical treadmill.
(B) Group-averaged phase maps from widefield responses to bilateral stimulus presentation moving along the azimuth (left hemispheres) or elevation (right hemispheres) before and after drug administration.
(C) Correlation coefficients for pre- versus post-phase maps across groups. Circles represent individual animals, and bars represent mean ± SEM.
(D) Widefield responses to grating patches presented to the right eye before and after drug administration during stationary periods. Inset shows cortical schematic with left visual areas in red.
(E) Cycle averages (top; gray bars represent stimulus period) and spatial spread of response (bottom) measured from a manually selected point in V1 (white asterisk, inset).
(F) Changes to visually evoked responses after drug administration across groups. Open circles represent individual animals; bars are mean ± SEM. A value of 1 represents no change, asterisks indicate significant change ($p < 0.05$; saline naive: $n = 5$; saline trained: $n = 5$; DOI naive: $n = 6$; DOI trained: $n = 5$).

Widefield imaging of cortical excitatory neurons in CaMKIIa-tTA:tetO-GCaMP6s mice (GCaMP6s mice; Wekselblatt et al., 2016) revealed no change in the retinotopic map of azimuth and elevation in visual cortex (Figures 1B and 1C; $p = 0.999$, Kruskal-Wallis; see also Movie S1) but a dramatic reduction in responses to grating patches in visual areas after DOI, but not saline, administration during stationary periods (Figures 1D and 1E). Interestingly, this reduction was larger in animals that had previously received training on a visual task than in animals naive to training (Figure 1F; $p = 0.012$, Kruskal-Wallis; paired t test: DOI trained: $p = 0.031$, $n = 5$; DOI naive: $p = 0.049$, $n = 6$; saline trained: $p = 0.192$, $n = 5$, saline naive: $p = 0.917$, $n = 5$). Passive stimuli used here were similar to those used in previous behavioral experiments (circular grating patches) but were different in size and location in visual space (see STAR Methods for further details), arguing against effects of perceptual learning. Furthermore, baseline responses between trained and naive animals were not statistically different (Figure S3).

DOI Reduces Surround Suppression in V1 L2/3 Excitatory Neurons

Given that widefield signals represent the summed activity in cell bodies, dendrites, and axons from many different excitatory cortical neurons, we next used two-photon calcium imaging to study the effect at the level of individual neurons, focusing on spatial integration. A key mechanism by which V1 neurons integrate information across space is through surround suppression, where larger stimuli tend to decrease V1 responses. This phenomenon can be explained by divisive normalization of "driving" classical receptive field (CRF) responses by "suppressive" responses in the extra-CRF (eCRF). We performed two-photon imaging in L2/3 of V1 in GCaMP6s mice while

showing grating patches of varying sizes (5°–50°), which revealed clear surround suppression in the neuropil responses (Figure 2A; see also Movie S2). Consistent with widefield imaging, DOI reduced the magnitude of visual responses at the level of neuropil, as well as the visual responses of individual neurons (Figure 2B). We computed size tuning curves from the individual neuron data (Figure 2C), fit these with a divisive normalization model (Ayaz et al., 2013; see STAR Methods), and measured the coefficients of the driving (R_D) and suppressive (R_S) fields. Both R_D and R_S were reduced after administration of DOI, but not saline (Figure 2D). These DOI-induced changes in R_D and R_S were significant for both naive and trained animals during stationary periods (Figure 2E; R_Dp = 0.021, R_S p = 0.010, Kruskal-Wallis; paired t test: DOI trained: R_D p = 0.003, R_S p = 0.002 n = 9/215; DOI naive: R_D p = 0.020, R_S p = 0.012, n = 8/144; saline trained: R_D p = 0.201, R_S p = 0.730 n = 11/197; saline naive: R_D p = 0.159, R_S p = 0.317, n = 11/269; where n = animals/cells; alpha = 0.025 corrected for multiple comparisons). DOI also reduced R_D during running bouts in trained, but not naive animals (not shown; R_D p = 0.023, R_S p = 0.032, Kruskal-Wallis; paired t test: DOI trained: R_D p = 0.015, R_S p = 0.026; DOI naive: R_D p = 0.084, R_S p = 0.357; saline trained: R_D p = 0.773, R_S p = 0.031; saline naive: R_D p = 0.744, R_S p = 0.559; alpha = 0.025 corrected for multiple comparisons).

Consistent with these changes in R_D and R_S, DOI reduced the suppression index in naive (stationary only) and trained (stationary and running) animals (Figures 2D and 2E; suppression index paired t test before versus after: DOI trained: p_{stat} = 0.005, p_{run} = 0.014; DOI naive: p_{stat} = 0.034, p_{run} = 0.814; saline trained: p_{stat} = 0.285, p_{run} = 0.150;

saline naive: p_{stat} = 0.261, p_{run} = 0.390).

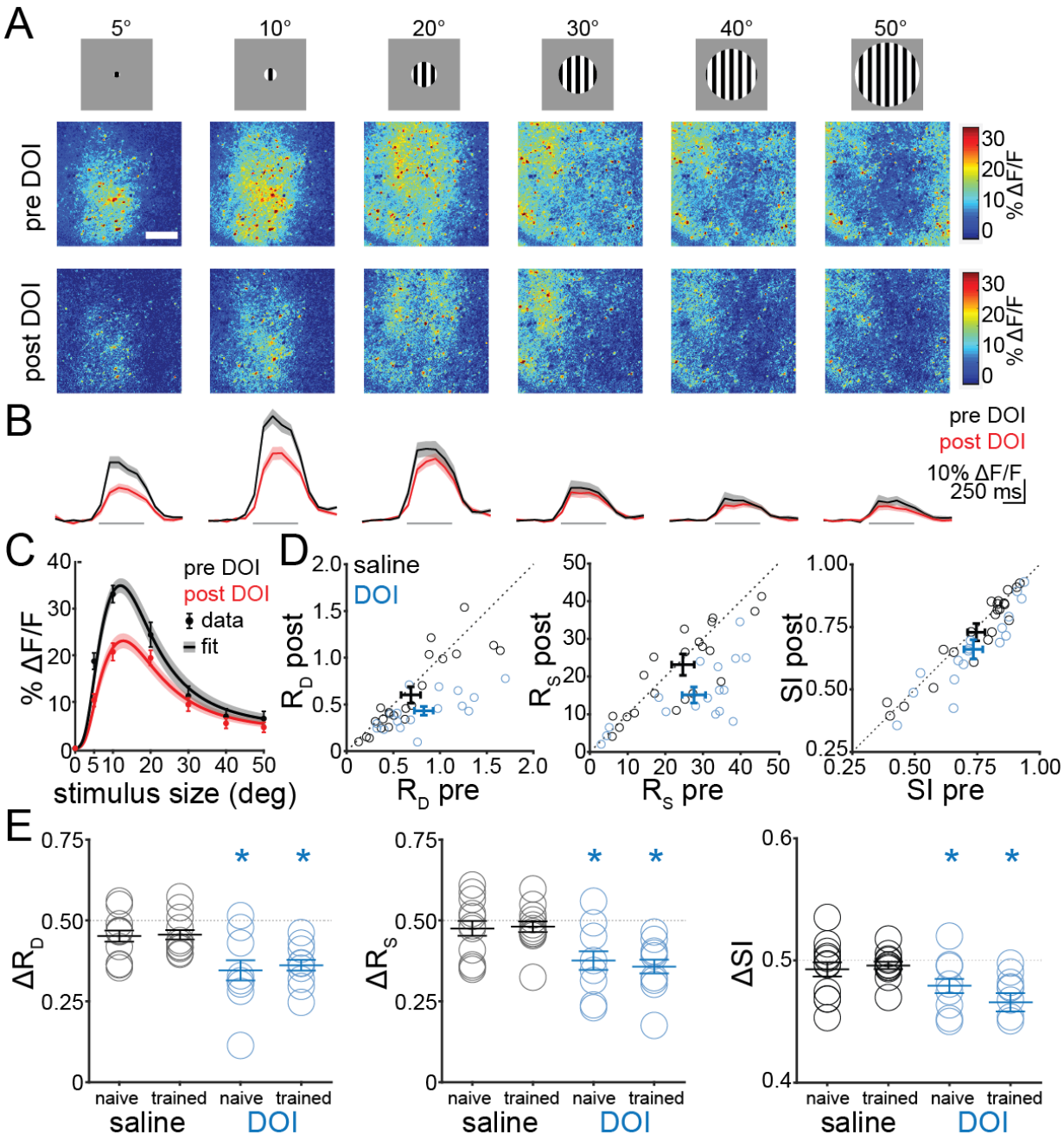

Figure 2. DOI Reduces Surround Suppression in V1 L2/3 Excitatory Neurons.

(A) Two-photon images in V1 showing responses to stimuli of increasing size before (top) and after (bottom) DOI administration in an example animal. Note surround suppression in the neuropil response. White scale bar in the top left image represents 200 μm. Data are from stationary periods only (see text for running data).

(B) Cycle averages of extracted (see STAR Methods) individual L2/3 excitatory neurons to corresponding stimuli shown above (gray bars show stimulus period), averaged within then across animals before (black) and after (red) DOI administration.
(C) Size tuning curve from data in (B) showing average responses of individual neurons with increasing stimulus size. Data are presented as points with error bars, and divisive normalization fits are shown as lines with shaded error bars.
(D) Driving (R_D) and suppressive (R_S) field coefficients and suppression index (SI) from divisive normalization fits of individual animal size-tuning curves for saline (black) and DOI (blue) before and after drug administration.
(E) Changes in driving and suppressive field coefficients and SI within each group before and after drug administration. A value of 1 represents no change, and asterisks indicate a significant change ($p < 0.025$ for R_D, R_S; $p < 0.05$ for SI; n = animals/cells: saline naive: n = 11/269; saline trained: n = 11/144; DOI naive: n = 8/144; DOI trained: n = 9/215).

DOI Reduces LFP Power and Bidirectionally Modulates Visually Evoked Firing Rate

In order to determine how 5-HT_{2A}R activation affects temporal dynamics of population activity, we recorded local field potentials (LFPs) using silicon probes and found the average LFP power in all cortical layers was reduced across a wide frequency range following administration of DOI in both spontaneous (not shown) and visually evoked activity (Figure 3A; paired t test, corrected for multiple comparisons: stationary saline: $p_{delta} = 0.184$, $p_{theta} = 0.531$, $p_{alpha} = 0.254$, $p_{beta} = 0.065$, $p_{gamma} = 0.0361$, n = 12 animals; stationary DOI: $p_{delta} = 0.127$, $p_{theta} = 0.0015$, $p_{alpha} = 0.002$, $p_{beta} = 0.0001$, $p_{gamma} = 0.0001$, n = 12 animals; running saline: $p_{delta} = 0.072$, $p_{theta} = 0.995$, $p_{alpha} = 0.572$, $p_{beta} = 0.616$, $p_{gamma} = 0.287$, n = 12 animals; running DOI: $p_{delta} = 0.766$, $p_{theta} = 0.0077$, $p_{alpha} = 0.02$, $p_{beta} = 0.0003$, $p_{gamma} = 0.0005$, n = 12 animals; alpha = 0.01). Interestingly, the visual stimulus-evoked increase in gamma power (28–35 Hz) was completely abolished after DOI administration. These results are consistent with findings from studies of hallucinogenic drug effects in humans using electroencephalography (EEG) and magnetoencephalography (MEG) (Kometer et al., 2013, Carhart-Harris et al., 2016), which also show an overall reduction in oscillatory synchronization.

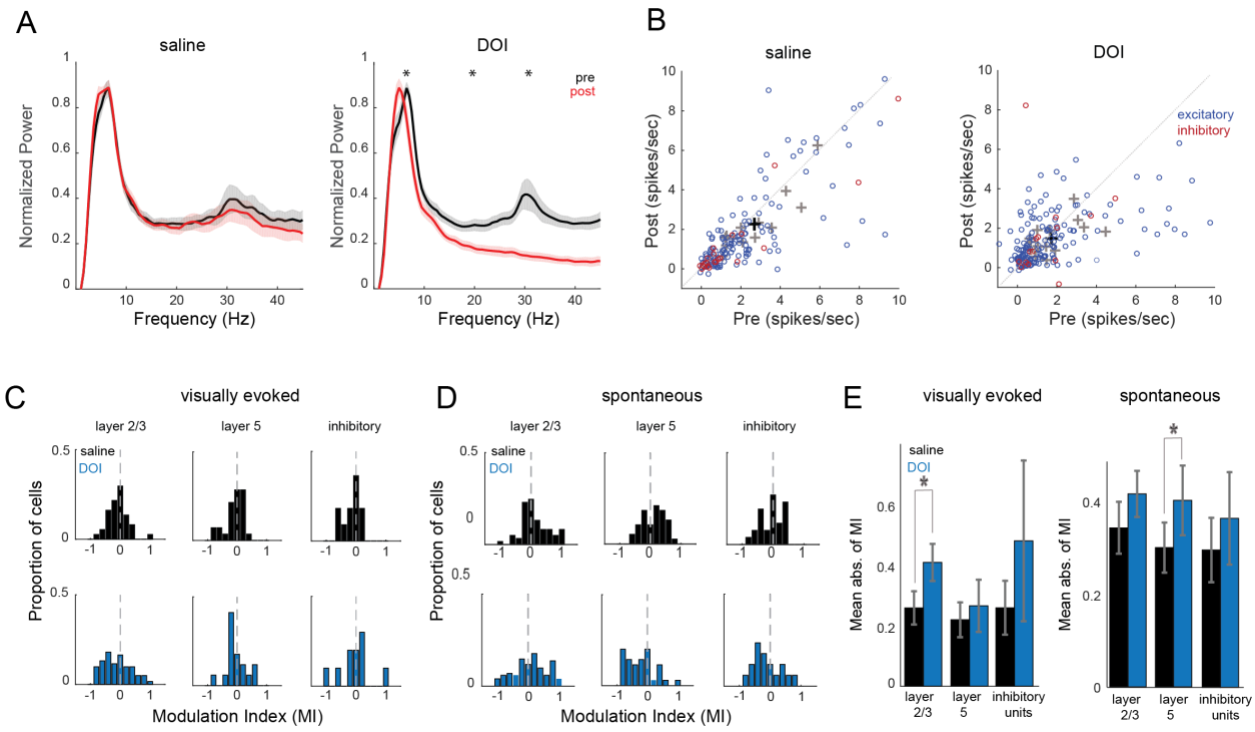

Figure 3. DOI Reduces LFP Power and Bidirectionally Modulates Visually Evoked Firing Rate.

(A) Average stationary and running LFP power ± SEM before (black) and after (red) administration of saline or DOI in response to sinusoidal drifting gratings (n_{saline} = 12 sessions, n_{DOI} = 12 sessions).
(B) Peak visually evoked firing rate before or after saline or DOI during stationary periods. Blue circles represent excitatory units, and red circles represent inhibitory units. 8% of saline units and 3% of DOI units are not shown. Black and gray crosses represent averages of all units and individual animals, respectively, including those not shown ($n_{saline\ exc}$ = 155 cells, $n_{saline\ inh}$ = 26 cells, n_{saline} = 15 animals, $n_{DOI\ exc}$ = 187 cells, $n_{DOI\ inh}$ = 17 cells, n_{DOI} = 15 animals).
(C) Change in peak firing rate as a function of initial peak firing rate. One saline and one DOI unit are not shown.
(D) Modulation indices (MIs) calculated from change in visually evoked peak firing rate between pre- and post-blocks. MI of 1 represents complete facilitation of firing rate after drug injection.
(E) MI distributions for spontaneous rates.
(F) Mean absolute value of MIs shows layer-specific changes between saline and DOI for the L2/3 evoked rate.

DOI Disrupts Temporal Dynamics in a Layer-Specific Manner but Maintains Tuning Properties

We next aimed to examine how individual V1 neuron activity is affected by 5-HT_{2A}R activation by analyzing responses of isolated single units to drifting sinusoidal gratings. We focused this analysis on L2/3 and L5 because they display distinct response properties (Niell and Stryker, 2008), and both excitatory and inhibitory neurons in these layers contain the highest 5-HT_{2A}R density in mouse neocortex (Weber and Andrade, 2010). Units were classified as putative excitatory or narrow-spiking inhibitory based on spike waveform (Niell and Stryker, 2008). As such, inhibitory neurons in this study are likely fast-spiking parvalbumin (PV) cells and not somatostatin (SOM)-expressing cells. Following DOI administration, the peak visually evoked firing rate of excitatory V1 neurons was bidirectionally modulated (Figure 3B; saline: $r_2 = 0.74$, $p = 0.679$, $n = 155$; DOI: $r_2 = 0.44$, $p = 0.181$, $n = 187$; paired t test). Interestingly, we observed rate-specific modulation of responses; neurons with initially low firing rates were facilitated, and neurons with initially high firing rates were suppressed (Figure 3C), similar to observations with 5-HT_{2A}R activation in anesthetized non-human primate and cat V1 (Watakabe et al., 2009, Rose and Horn, 1977). In contrast to the excitatory neuron population, inhibitory neurons did not change their peak evoked firing rate (saline: $r_2 = 0.73$, $p = 0.103$, $n = 26$; DOI: $r_2 = 0.93$, $p = 0.812$, $n = 17$; paired t test). The same pattern was observed during locomotive states (not shown; saline excitatory: $r_2 = 0.55$, $p = 0.057$, inhibitory: $r_2 = 0.75$, $p = 0.215$; DOI excitatory: $r_2 = 0.44$, $p = 0.7.15e-05$, inhibitory $r_2 = 0.93$, $p = 0.577$; paired t test).

To determine how strongly each cortical layer was affected by DOI, we calculated modulation indices of stationary peak firing rate across the neural population, where negative (positive) values represent neurons that reduced (increased) their rate following drug administration (Figures 3C and 3D). The distributions were shifted overall toward suppression; however, because these distributions were bidirectional, we calculated the mean absolute value for each layer to determine the strength of modulation independent of sign. This revealed visually evoked responses in L2/3 were more affected by DOI than saline (t test: $p = 0.005$, corrected for multiple comparisons), whereas spontaneous rate was not affected (Figure 3E). Thus, the effects of DOI are specific for layer and cell type and differ for spontaneous versus evoked activity.

We next determined how DOI affected the time course of V1 responses based on the peristimulus time histogram (PSTH) of responses to drifting gratings (Figure 4A). Following DOI administration, we saw layer-specific changes in the mean PSTH of visually responsive cells (neurons with peak visually evoked rate greater than 2 Hz in either the pre- or post-recording block). The mean response of both L2/3 and L5 was significantly reduced (two-sample Kolmogorov-Smirnov test; L2/3: $p_{stat} = 0.0001$, $n = 37$, $p_{run} = 0.004$, $n = 61$; L5: $p_{stat} = 0.001$, $n = 13$, $p_{run} = 0.026$, $n = 19$), consistent with more neurons being suppressed than enhanced, whereas inhibitory units were not affected (inhibitory [inh.]: $p_{stat} = 0.878$, $n = 7$, $p_{run} = 0.878$, $n = 10$).

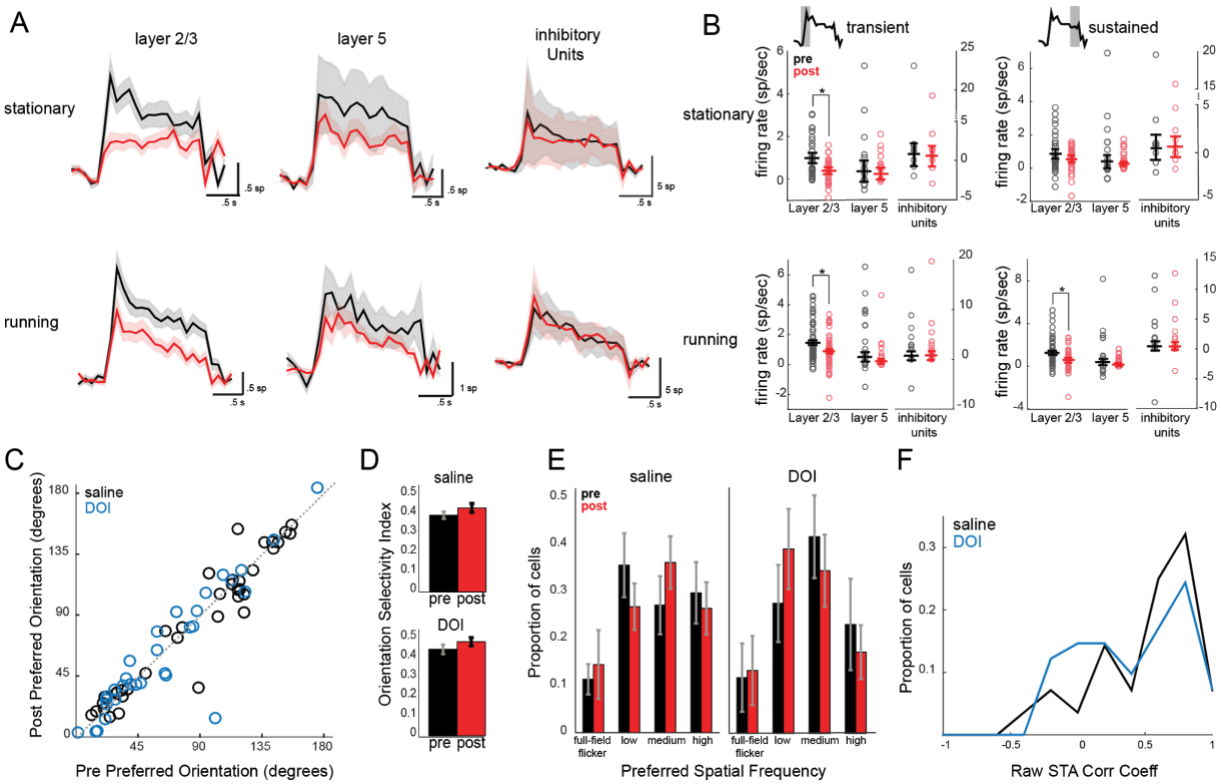

Figure 4. DOI Disrupts Temporal Dynamics in a Layer-Specific Manner but Maintains Tuning Properties.

(A) Mean peristimulus time histograms ± SEM before (black) and after (red) administration of DOI across L2/3, L5, and inhibitory units during stationary and locomotive periods. Gray bars show stimulus period.
(B) Mean firing rate for each cell before or after DOI administration across transient and sustained components from PSTHs shown in (A). The transient component is defined as the first 500 ms after stimulus onset, and the sustained component is defined as the 500 ms preceding the stimulus offset (L2/3: n_{stat} = n = 37, n_{run} = 61; L5: n_{stat} = 13, n_{run} = 19; inh. n_{stat} = 7, n_{run} = 10).
(C) Preferred orientation of individual neurons before or after saline or DOI administration (n_{saline} = 37, n_{DOI} = 33).
(D) Average orientation selectivity index (OSI; circular variance) across populations of visually responsive cells before or after saline or DOI injection (n_{saline} = 100, n_{DOI} = 91).
(E) Proportion of visually responsive cells (>2 Hz) selective for preferred spatial frequencies before or after drug treatment (n_{saline} = 100, n_{DOI} = 93).
(F) Histograms of 2D correlation coefficients of raw spike triggered average receptive fields of all cells responsive above 2 Hz. A value of 1 represents STAs that did not change after saline or DOI administration (n_{saline} = 28, n_{DOI} = 41).

The time course of the mean PSTH showed a transient response at stimulus onset followed by a smaller sustained response, which was most pronounced in L2/3 neurons (Figure 4A). Notably, the transient (first 500 ms after stimulus onset) and sustained (500 ms preceding stimulus offset) components were differentially affected by DOI. We separated the two temporal components and found that L2/3 was strongly suppressed during the transient component (p_{stat} = 0.0002, p_{run} = 0.0035) and was only affected during the sustained component when animals were running (p = 0.0007; Figure 4B). L5 and inhibitory units, in contrast, did not show a significant net change in either temporal component ($L5_{trans}$ p_{stat} = 0.0471; $L5_{trans}p_{run}$ = 0.864; $L5_{sus}$ p_{stat} = 0.436; $L5_{sus}$ p_{run} = 0.727; inh_{trans} p_{stat} = 0.587; inh_{trans} p_{run} = 0.875; inh_{sus} p_{stat} = 0.964; $inh_{sus}p_{run}$ = 0.852). Thus, DOI administration disrupts temporal dynamics of visual responses in L2/3 by strongly reducing the onset transient.

We next determined if DOI affected the encoding of low-level stimulus features and feature selectivity. Across the recorded population of neurons, we found no change for the preferred grating orientation following DOI administration (Figure 4C; saline: r_2 = 0.92, p = 0.346, n = 37; DOI: r_2 = 0.87, p = 0.639, n = 33; not shown; saline running: r_2 = 0.87, p = 0.425, n = 27; DOI running: r_2 = 0.81, p = 0.873, n = 43; paired t test). The mean orientation selectivity index was also unaffected by DOI and saline administration (Figure 4D; Wilcoxon rank sum test on mean of stationary and running; saline: p = 0.362, n = 100; DOI: p = 0.214, n = 91). Preferred direction of grating motion and mean direction selectivity index (DSI) were also unchanged (not shown; Wilcoxon rank sum test; preferred direction saline stationary: r_2 = 0.95 p = 0.912 n = 33, running: r_2 = 0.5 p =

0.929 n = 25; DOI stationary: r_2 = 0.57 p = 0.861 n = 56; running: r_2 = 0.46 p = 0.486 n = 62; DSI saline stationary: p = 0.95 n = 71; running: p = 0.25 n = 71; DOI stationary: p = 0.33, n = 64; running: p = 0.70, n = 64). We also found no change in the distribution of spatial frequency preference for responsive cells, as the same proportions were selective to either low (0.01–0.02 cycles per degree [cpd]; paired t test mean of running and stationary; saline: p = 0.435; DOI: p = 0.823), medium (0.04–0.08 cpd; saline: p = 0.334; DOI: p = 0.397), or high (0.16–0.32 cpd; saline: p = 0.640; DOI: p = 0.485) spatial frequencies or to full-field flicker (saline: p = 0.267, DOI: p = 0.577) following DOI treatment (Figure 4E; saline: n = 100; DOI: n = 93). The observed changes in firing rate did not correlate with tuning properties or selectivity (not shown; saline preferred [pref] orientation [ori] stationary [stat]: r_2 = 0.012, pref ori moving [mv]: r_2 = 0.034, orientation selectivity index [OSI] stat: r_2 = 0.005, OSI mv: r_2 = 0.063; DOI: pref ori stat: r_2 = 0.0001; pref ori mv: r_2 = 0.0096; OSI stat: r_2 = 0.021; OSI mv: r_2 = 0.053).

To determine the similarity in receptive field structure before and after treatment, we calculated 2D correlation coefficients between raw spike-triggered average receptive fields (STAs) computed from pre- and post-recording sessions. We found no significant differences between the distributions of coefficients calculated from saline and DOI recording blocks (Figure 4F; two-sample t test: p = 0.348, n_{saline} = 28, n_{DOI} = 41). Thus, despite significant changes in temporal dynamics and spatial contextual modulation, basic tuning properties and receptive field structure of individual V1 neurons were unchanged after 5-HT_{2A}R activation.

DISCUSSION

Using widefield and two-photon calcium imaging and single-unit electrophysiology in awake mouse V1, we investigated how systemic administration of the hallucinogenic 5-HT_{2A}R agonist DOI affects cortical processing of visual information. We found reductions in response gain and surround suppression and altered temporal dynamics but no changes in basic tuning properties. Together, this study provides a systematic measurement of the effects of hallucinogenic 5-HT_{2A}R agonist administration on visual coding of cortical sensory neurons in awake animals.

It remains to be determined whether the observed effects are due to action on 5-HT_{2A}Rs within V1 or elsewhere. Watakabe et al. (2009) administered DOI locally through microinfusions in V1 and also observed bidirectional firing rate modulation, suggesting that 5-HT_{2A}R activation in V1 is sufficient to drive neurophysiological changes consistent with systemic DOI administration. It is unknown, however, if local action of 5-HT_{2A}Rs in V1 alone is sufficient to drive perceptual changes. Furthermore, the circuit mechanisms by which these 5-HT_{2A}R-mediated changes occur are unclear. Evidence also suggests that other members of the 5-HT_2 receptor family are activated by DOI, albeit with significantly lower efficiency, and DOI is more selective for 5-HT_{2A}R than LSD (Knight et al., 2004). Given that our dose is comparable to most studies of 5-HT_{2A}R function (see Methods for discussion), we do not expect this to be the case; however, we cannot rule out that 5-HT_{2B} or 5-HT_{2C} receptors contribute to our results. These issues will be important to address in future studies of psychedelic drug influence on sensory cortical processing.

5-HT$_{2A}$R Activation Reduces Sensory Drive

Models of hallucination suggest that reductions in bottom-up sensory drive can lead to a misinterpretation of sensory information. We observed reduced visually evoked widefield calcium activity, a measure of bulk activity in excitatory neurons, suggesting 5-HT$_{2A}$R activity reduces sensory drive in cortex. At the level of individual neurons, DOI administration bidirectionally modulated firing rates, but the overall effect was a decrease in V1 responses, which has also been observed in anesthetized primates and cats (Watakabe et al., 2009, Dray et al., 1980, Rose and Horn, 1977). Reduced sensory drive may lead to increased dependence on top-down expectations, leading to misinterpretation of sensory information, as hypothesized by current models of hallucination (Cassidy et al., 2018, Grossberg, 2000).

Previous *in vivo* studies have not discriminated between excitatory or inhibitory cell types or cortical layers in the context of 5-HT$_{2A}$R modulation of V1 response properties. Both excitatory and inhibitory populations showed bidirectional changes after DOI administration, though inhibitory neuron changes were not significant, possibly due to small sample size. Furthermore, 5-HT$_{2A}$R activation resulted in layer-specific modulation of excitatory neuron activity, decreasing evoked responses in L2/3. Given that subsets of excitatory and inhibitory neurons express 5-HT$_{2A}$Rs, with a majority in L5 (Weber and Andrade, 2010), it is possible that the directionality of DOI-induced change in a neuron's visual response is determined by whether it expresses 5-HT$_{2A}$R rather than its excitatory or inhibitory identity. Current evidence points toward increased excitability in 5-HT$_{2A}$R-

expressing neurons (Avesar and Gulledge, 2012, Stephens et al., 2014), suggesting that non-expressing neurons, the majority of V1, may be suppressed via network mechanisms.

A recent study (Seillier et al., 2017) observed changes in visual responses after local iontophoresis of 5-HT into macaque V1 that were quite similar to those seen here, including a net decrease in response gain without change in selectivity, despite the fact that 5-HT itself acts on multiple receptor subtypes in cortex. Together, our findings suggest that at least in visual cortex the effect of 5-HT is dominated by the 2A subtype; however, future studies could further examine how different serotonin receptor subtypes contribute to modulation of sensory processing. Addressing these questions will require reliable genetic access to 5-HTR-family expressing neurons, which would also permit manipulations to determine the specific circuits mediating the effects observed here (Gong et al., 2007).

5-HT$_{2A}$R Activation Alters Visual Contextual Modulation in Excitatory V1 Neurons

Beyond CRF properties, contextual influences are critical components of visual processing. Lateral and top-down connections are thought to be key mediators of contextual processing, which is important for perceptual functions such as attention and figure-ground segregation. Disrupted contextual processing, including decreased visual surround suppression at the psychophysical and physiological levels, has been reported in patients with schizophrenia (Butler et al., 2008, Tibber et al., 2013, Zenger-Landolt and Heeger, 2003). Failure to appropriately incorporate contextual information could also underlie altered visual perception observed with psychedelic drugs. We found reduced

surround suppression in V1 neurons resulting from decreased strength of driving and suppressive field coefficients after 5-HT$_{2A}$R activation, consistent with studies in patients with schizophrenia. This suggests these receptors may be important for adjusting the influence of context in visual cortical processing.

The magnitude of DOI-induced change in some measures was larger for trained than naive animals, including the amplitude of responses measured with widefield imaging and the suppressive field measured with two-photon imaging. Given that pupil diameter and time spent running did not consistently change after DOI administration (Figure S2), we do not anticipate changes seen here reflect solely changes in behavioral state or depth of field. Training on a visual task can result in a variety of changes in visual cortical processing, such as stimulus prediction or expectation, attention, stimulus encoding, and perceptual learning (for review, see Khan and Hofer, 2018). These learning-induced changes can be context specific and dependent on either bottom-up or top-down inputs. The various inputs to V1 that are modified by different learning paradigms could be differentially affected by neuromodulators, and untangling the logic of 5-HT$_{2A}$R modulation of specific V1 inputs may lend insight into the mechanisms of learning-induced changes in V1.

5-HT$_{2A}$R Activation Disrupts Temporal Dynamics of Visual Responses

DOI disrupted temporal dynamics at the population level, where we observed decreases in LFP power, and at the single-unit level, where we observed strong suppression of the transient onset response in L2/3 neurons. Previous studies suggest the transient

component of visual responses are more weakly tuned than sustained responses (Ringach et al., 1997) and that transient responses may encode behaviorally relevant signals such as salience, novelty, or expectation (Homann et al., 2017, Fiser et al., 2016). Sustained responses may more accurately encode stimulus identity. We found that 5-HT2AR activation differentially affected these response components in a cell-type- and layer-specific manner. Specifically, DOI altered transient responses in excitatory, but not inhibitory, L2/3 neurons, whereas sustained responses were unaffected. Given the relatively small effects of DOI on sustained relative to transient responses, along with the maintenance of feature selectivity in V1 neurons, these data suggest 5-HT2AR activation does not disrupt stimulus encoding at the level of individual neurons but rather alters integration of top-down with bottom-up sensory information.

We also observed changes in temporal dynamics at the population level as a dramatic 5-HT2AR-mediated decrease in visually evoked LFP power across V1 layers. Patients with schizophrenia (Uhlhaas and Singer, 2010, Moran and Hong, 2011) and subjects administered psychedelic drugs (Liechti, 2017) display reduced oscillatory power specifically in the gamma frequency band, which is associated with neuronal responses to visual stimuli (Liechti, 2017, Sedley and Cunningham, 2013) and communication across neural populations through coordinated activity (Jia et al., 2013). Additionally, animal models of hallucination show reduced oscillatory synchronization across various brain areas (prefrontal cortex [PFC]: Wood et al., 2012, Celada et al., 2008; nucleus

accumbens: Goda et al., 2013; hippocampus, striatum, and reticular formation: Dimpfel et al., 1989).

Implications for Models of Hallucination and Sensory Processing

Despite these DOI-mediated changes in V1 sensory drive and temporal dynamics, CRF tuning properties and stimulus encoding remained unchanged. This suggests that altered visual perception related to 5-HT$_{2A}$R function results not from changes in V1 stimulus encoding but from impaired downstream integration due to changes in gain and temporal dynamics. Consistent with these findings, many perceptual deficits in patients with schizophrenia are attributed to reduced gain of sensory responses (Butler et al., 2008, Phillips and Silverstein, 2013).

Understanding the action of 5-HT$_{2A}$Rs may provide insight into the general principles of cortical sensory processing, particularly given the potent impact of hallucinogenic 5-HT$_{2A}$R agonists on perception and cognition. There is increased urgency for understanding the neurophysiological effects of 5-HT$_{2A}$R modulation given the recent resurgence in use of psychedelic drugs in the treatment of mental health disorders (Johnson and Griffiths, 2017, Carhart-Harris and Goodwin, 2017). Our results provide a basis for investigating circuit-specific actions of these drugs in cortical function.

CHAPTER III

BINOCULAR GAZE STABILIZATION DURING PREY CAPTURE IN FREELY MOVING MICE

ABSTRACT

Many studies of visual processing are conducted in unnatural conditions, such as head-and gaze-fixation. However, this radically limits natural exploration of the visual environment, which is naturally achieved through directed eye, head, and body movements. Though head-fixed studies have lent insight into visual feature encoding under stationary viewing conditions, there is much less known about how animals actively use their sensory systems in natural contexts to acquire visual information about the world. Recently, capture of insect prey by mice has emerged as an ethologically relevant behavioral paradigm that mice perform under natural conditions. Though this behavior is visually mediated, it is unclear what behavioral strategies mice use to localize moving prey in their visual field to allow for accurate approach and capture, particularly since mice, unlike most predators, lack foveate vision and have a relatively narrow binocular field. To this end, we have recorded bilateral eye movements while unrestrained mice approach and capture live insect prey. This is achieved using a set of miniature cameras that are reversibly mounted to the mouse's head, together with an overhead camera to record movements of the mouse and cricket. We find that upon selection of the visual target (cricket), the eyes rapidly move in the same direction as the head (i.e., saccade), quickly shifting the gaze direction to the new location. Then, during pursuit ongoing eye movements counter-act head movements to stabilize the visual field and re-center the eyes as necessary, effectively fixing the gaze and binocular zone over

the new visual target location. Despite afoveate vision and a narrow binocular field, mice actively control eye movements to achieve visually-mediated behaviors.

INTRODUCTION

Across animal species, eye movements are used to acquire information about the world, and vary based on the particular goal (Yarbus, 1967). Mice, currently the most commonly utilized model system to study visual processing, use visual cues to successfully achieve goal directed tasks in freely-moving behavioral paradigms in both artificial and ethologically relevant contexts (e.g., Morris water maze, nest building, prey capture; (R. G. M. Morris 1981, Clark, Hamilton, and Whishaw 2006, Hoy et al. 2016). It is unclear however, how this is achieved because mice lack foveate vision and have laterally facing eyes, and as a consequence, a relatively limited binocular field (roughly 40° in mice, as opposed to 135° in humans; Drager 1978). As such, it is unclear if mice regulate their gaze during locomotion to track moving visual targets. Therefore, we aimed to determine what oculomotor strategies allow for effective tracking of moving prey during free movement. More broadly, we aimed to understand the coordination of eye and head movements in the context of self-motion in an afoveate and binocularly limited species.

Typically predators have front-facing eyes which creates wide binocular fields, allowing for depth perception and effective hunting. In contrast, prey typically have lateral facing (and more mobile) eyes, and thus large monocular fields, which allows reliable motion detection of approaching predators in the periphery (Cartmill, 1974). Mice, generally thought of as prey animals, can act like predators, even though they have

these characteristics of prey. How then are animals with limited monocular overlap able to localize moving visual targets directly in front of them, especially with a narrow binocular field and while lacking a fovea? This would require the ability to modulate the amount of monocular overlap to generate a larger binocular field, through directed eye movements (such as in the case of starlings and chameleons), or the use of coordinated head and eye movements to direct, center, and stabilize the binocular field over the visual target.

Eye movements in head-restrained rodents are limited relative to eye movements in freely moving rodents (Wallace et al. 2013, Payne and Raymond 2017, Meyer et al., 2018), potentially due to VOR-compensation from head movements. As such, using miniaturized cameras along with an overhead camera, we designed a system to record head and bilateral eye movements while unrestrained mice performed a visually guided and goal-directed task, approach and capture of live insect prey. We compared the coordination of eye and head movements during approach and non-approach epochs to determine what oculomotor strategies mice use to pursue and capture prey.

MATERIALS AND METHODS

Animals and behavioral habituation

All procedures were conducted in accordance with the guidelines of the National Institutes of Health and were approved by the University of Oregon Institutional Animal Care and Use Committee. Animals used for this study were wild-type (C57 Bl/6J) males and females aged 2-6 months. At 2 months of age, the animals began the habituation

process. They were first handled by the experimenters for at least 6 3-minute sessions over 1-2 days. Following handling, the animals were placed in the prey capture arena to explore with their cagemates. The duration of this stage of habituation was at least 6 10-minute sessions over 1-2 days. One cricket (Rainbow mealworms, 5-week old) per mouse was placed in the arena with the mice for the last half of the habituation sessions. One cricket per mouse was then placed in the homecage overnight for additional practice. For the subsequent habituation step, the mice were placed in the arena alone with one cricket for 7-10 minutes. This step was repeated for 2-3 training days (6-9 sessions) until most mice successfully caught crickets within the 10-minute period.

Animals were then habituated to head-fixation above a spherical Styrofoam treadmill (Dombeck et al. 2007). Headfixation was only used to fit and adjust cameras. Cameras were then fitted to each mouse (described below) and mice were habituated to wearing the cameras while walking freely in the arena. After the animals were habituated to the arena while wearing cameras, they were habituated to hunting with cameras attached. This took roughly 1-2 10 minute sessions for each mouse. The animals were then food deprived for a period of ~18 hours and then run in the prey capture assay for 3 10-minute sessions per data collection day. Animals readily capture crickets in their homecage without training or food deprivation but food deprivation allows for more trials within the experimental arena.

The rectangular prey capture arena is a white arena of dimensions 38 x 45 x 30 cm (Hoy et al. 2016). The arena was illuminated with one 15 Watt, 100 lumen incandescent light bulb placed roughly 1 meter above the center of the arena to mimic lux

during dawn and dusk, times at which mice naturally hunt. Video signal was recorded from above the arena using a CMOS camera (Basler Ace, acA2000 – 165 umNIR, 30 Hz acquisition).

Surgical procedure

Before the habituation process, mice were surgically implanted with a steel headplate to allow for head-fixation during camera adjustment (Niell and Styker, 2010). Animals were anesthetized with isoflurane (3% induction, 1.5%–2% maintenance, in O_2) and body temperature was maintained at 37.5°C using a feedback-controlled heating pad. Fascia was cleared from the surface of the skull following scalp incision and a custom steel headplate was attached to the skull using Vetbond (3M) and dental acrylic. The headplate was placed near the back of the skull, roughly 1 mm anterior of Lambda. A flat layer of dental acrylic was placed in front of the headplate to allow for attachment of the camera connectors. Carprofen (10 mg/kg) and lactated Ringer's solution were administered subcutaneously and animals were monitored for three days following surgery.

Camera assembly and head-mounting

Cameras used in this study were 6 x 6 x 6 mm (iSecurity101) with a resolution of 480x640 pixels and a 78 degree viewing angle. A 200 Ohm resistor and 3mm IR LED were integrated onto the cameras for uniform illumination of the eyes. Power, ground, and video cables were soldered with lightweight 36 gauge FEP hookup wire (Cooner Wire; CZ 1174). A 6 mm diameter collimating lens with a focal distance of 12 mm (Lilly

Electronics) was inserted into custom 3D printed housing and the cameras were then inserted and glued behind this (see Figure 1 for schematic of design). The inner side of the arm of the camera holder housed a connector (Mill-Max Manufacturing Corp. 853-93-100-10-001000) cut to 5mm (2 rows of 4 columns). This connector is used for reversible attachment of the cameras to the implants of experimental animals. The total weight of the two cameras, with the lenses, connectors, and 3D printed holder is 2.6 grams.

Following camera assembly, connectors were bilaterally fitted onto the mice using the corresponding female sockets. When the camera was appropriately focused on the eye, the connectors were glued onto the acrylic implant using cyanoacrylate adhesive (Loctite).

Behavioral Experiments

Following the habituation process, mice were food deprived for ~18 hours then placed in the arena for prey capture behavior. Each day of data collection was 3 10-minute sessions per mouse. Mice were placed in the prey capture arena with one cricket following camera attachment. Experimental animals captured and consumed the cricket before a new cricket was placed in the arena. The experimenters removed any residual cricket pieces in the arena before the addition of the next cricket. A typical mouse catches and consumes between 3-5 crickets per 10 minute session. Video data as well as timestamps for the two eyes and overhead arena camera were acquired at 30 frames per second using Bonsai (Lopes et al. 2015). Control experiments were performed using the

same methods, but with no cameras attached.

Eye, head, and body tracking

DeepLabCut (Mathis et al. 2018) was used for markerless estimation of eye position and mouse and cricket position. For DeepLabCut training, we selected 8 points on the mouse head (nose, two camera connectors, two IR LEDs, two ears, and center of the head between the two ears), and two points for the cricket (head and body). Following estimation of the selected points, analysis was done in custom MATLAB scripts.

Position and angle of the head were computed by fitting the 8 measured points on the head for each video frame to a defined mean geometry plus and x-y translation and horizontatl rotation. The head direction was defined as the angle of this rotation, referenced to the line between the nose and center of the head. We defined approaches as times at which the velocity of the mouse was greater that 5cm/sec, the heading of the mouse was between -45 and 45 degrees relative to cricket location, and the distance to the cricket was decreasing at a rate greater than 5 cm/sec.

Ellipse fitting and eye camera calibration

Using DeepLabCut (Mathis et al., 2018), eight points along the edge of the pupil were extracted and tracked through the video sequence. The eight points were then fit to an ellipse using the least squares criterion. The general form of calibration and pupil tracking then followed methods used in Wallace et al., 2013. Briefly, this approach is based on the fact that when the eye is looking directly on the camera axis the pupil will appear circular, and as the eye rotates the circular shape will flatten into an ellipse depending on the direction and degree of angular rotation from the center of the camera

axis. Two pieces of information are needed to calculate the transformation of a circle along the camera axis to the ellipse fit: the camera axis center position and the scale factor relating pixels of displacement to angular rotation. To find the camera axis, following Wallace et al., 2013, we used the constraint that the major axis of the pupil ellipse will be perpendicular to the vector from the pupil center to the camera axis center. This defines a set of linear equations for all of the pupil observations with significant ellipticity, which can be solved directly with a least squares solution. Next, the scale factor was estimated based on the equation defining how much the ellipticity of the pupil changes with the corresponding shift from the camera center in each video frame. Based on the camera center and scale factor for each video, we calculated the affline transformation needed to transform the circle to the ellipse fit of the pupil in each frame and the angular displacement from the camera axis was then used for subsequent analyses. Mathematical details of the methods are presented in Wallace et al., 2013.

Following computation of kinematic variables (mouse, cricket, and eye position/rotation), these values were linearly interpolated to a standard 30Hz timestamp to account for small differences in video acquisition timing.

RESULTS

Reversibly Attached Head Mounted Cameras Do Not Hinder Hunting Ability

To determine which visuomotor strategies are used to track prey, mice hunted live crickets in an experimental arena while wearing reversibly attached, laterally placed head-mounted cameras (Figure 1A, 1B). The miniaturized eye-tracking cameras were fitted into a custom design 3D printed holder that also housed a collimating lens to focus

on the eye and connectors for reversible attachment to the implants of experimental animals (Figure 1C). The cameras did not affect overall mouse velocity in the arena or total number of crickets caught per 10-minute session (paired t-test, p=.075; Figure 1E), suggesting that placement of the cameras did not occlude important segments of the visual field required for successful prey capture behavior. Performance of experimental animals steadily improved over the course of several 10-minute sessions and there was no noticeable difference in learning or performance between male and female mice (Figure 1F; paired t-test, p=.304).

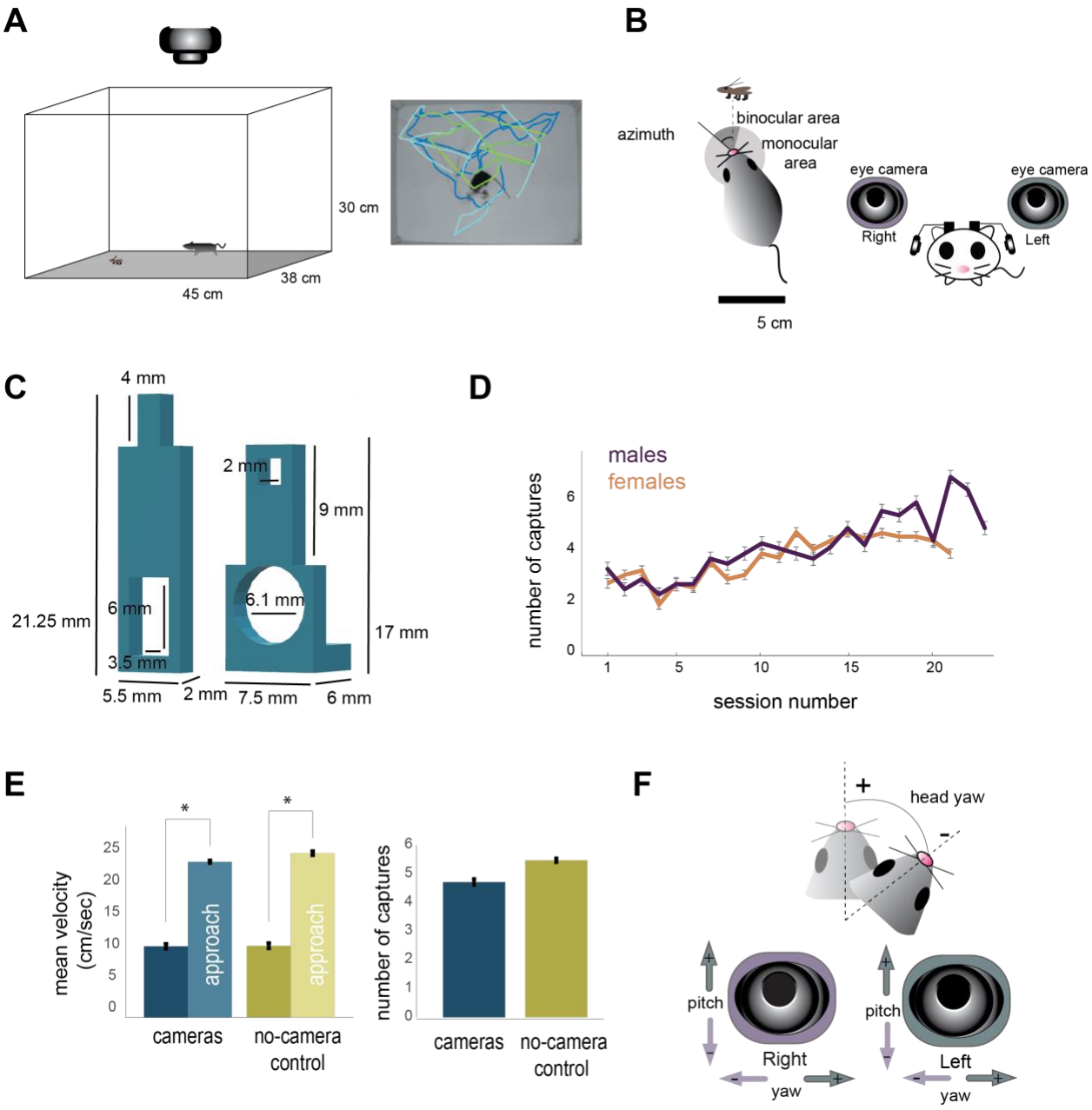

Figure 5. Reversibly Attached Head Mounted Cameras Do Not Hinder Hunting Ability.

(A) Unrestrained mice hunted live crickets in a rectangular plexiglass arena. Using an overhead camera, we tracked movement of the mouse and cricket. Example tracks of mouse (blue), cricket (cyan), and mouse during approach (green).
(B) Mice have a narrow binocular field and wide monocular fields, requiring a strategy for maintaining moving targets in front of their heads while hunting. We calculated azimuth (horizontal angle to cricket). Reversibly attached cameras were bilaterally placed on the head of experimental animals while they performed prey capture behavior.

(C) Schematic of custom-design 3D printed lens and camera holder. The left piece is inserted into the piece on the right. The connector that attaches to the implant on the animal fits into the rectangular hole on the left piece.
(D) We calculated horizontal angular movements of the head and eyes (yaw), where positive yaw is counterclockwise to the mouse when viewed from above (towards the temporal side of the mouse's left eye). Vertical angular positions of the eyes (pitch) were also calculated, with positive values above the centroid.
(E) Attachment of cameras did not affect average mouse velocity in the experimental arena. Approach velocity was significantly greater than non-approach velocity with and without cameras attached. Number of captures per session with cameras did not vary from number of captures without cameras ($n_{cameras}$=10 animals, 302 trials, $n_{control}$=10 animals, 263 trials). Bars represent mean ± SEM.
(F) Average number of captures per 10-minute session with cameras attached steadily increased and did not vary between male and female animals (n_{males}=5, $n_{females}$=6). Bars represent mean ± SEM.

Along with an overhead camera, we recorded the behavior of experimental animals and the cricket prey. We defined points on the head, cricket, and eyes for markerless point estimation using DeepLabCut (Mathis et al. 2018), then calculated angular positions of horizontal head and eye position (yaw) and vertical eye position (pitch) using these points (Figure1D). With these measures, we sought to understand the coordination of eye and head movements during a visually guided, goal-directed, and ethologically relevant behavior, prey capture.

Eye position is more bilaterally centered during approach periods.

We first aimed to characterize the coordination of bilateral eye movements, regardless of changes in head position. We observed that the two eyes typically maintain a linear relationship between horizontal and vertical position during free movement (Figure 2A), and that the two eyes, in both yaw and pitch positions, are more centrally located during approach periods relative to non-approach time points (Figure 2A, 2B; paired t-test p_{yaw}<.001; p_{pitch}<.001). Interestingly, comparing the yaw eye positions

between the two eyes showed that roughly half of eye movements during non-approach periods are congruent (move in the same direction), and that this relative proportion significantly increases during approach periods (paired t-test, $p<.0001$). In contrast, the proportion of incongruent (i.e., convergent and divergent) eye movements decreases during approach periods (Figure 2D) (paired t-test, $p_{convergent}=.0016$, $p_{divergent}<.001$). Additionally, the distribution of differences in yaw between the two eyes was also closer to 0 during approach epochs (Figure 2E; paired t-test, $p<.001$). As a whole, eye position is more centered during approach periods, whereas eye movements during non-approach periods are more variable potentially due to head movements.

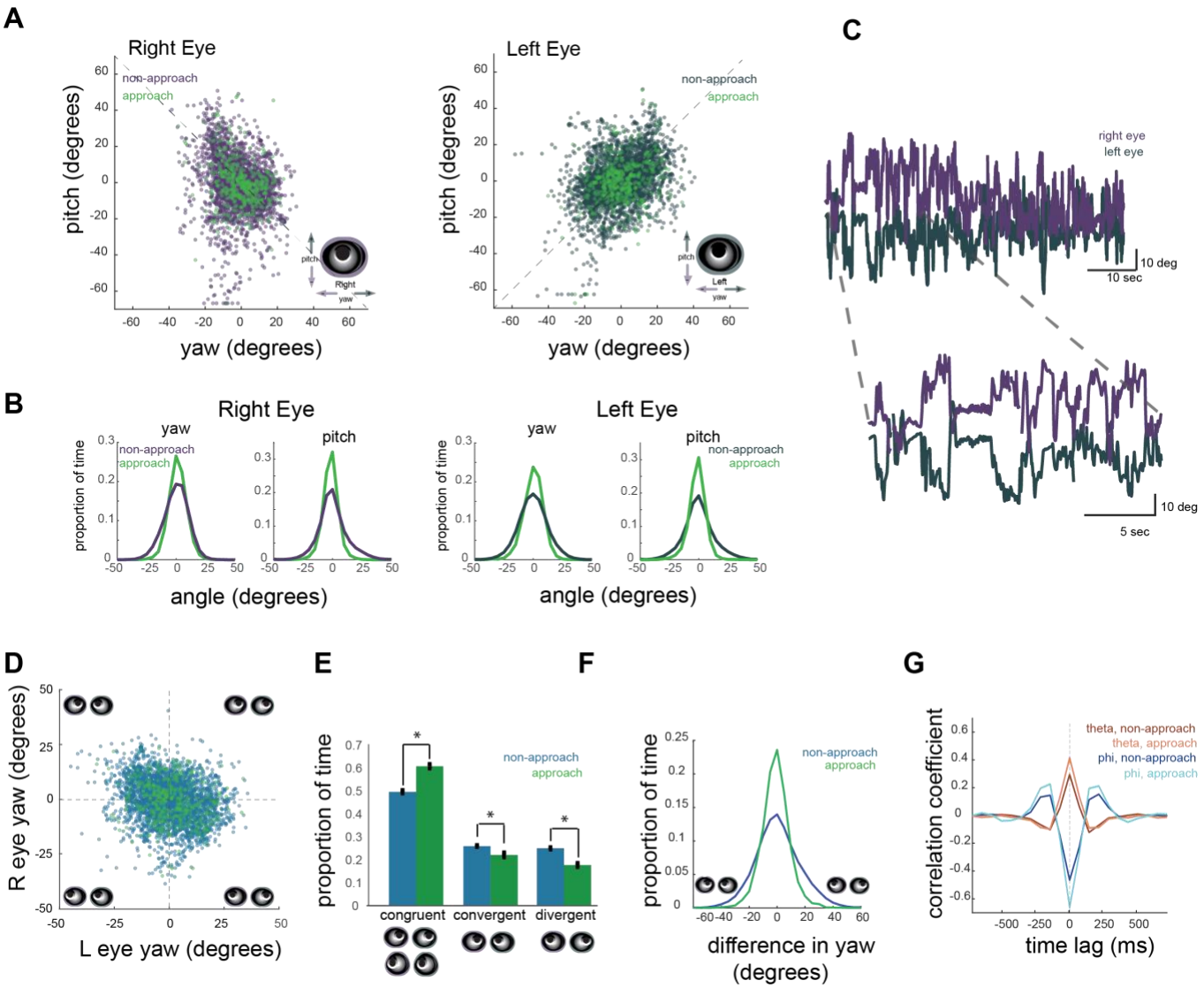

Figure 6. Eye position is more bilaterally centered during approach periods.

(A) Yaw and pitch eye positions at non-approach and approach times for right (purple) and left (teal) eyes. Green points represent points during approaches ($n_{animals}$=8, n_{trials}=302).
(B) Histograms corresponding to data in A where proportion of eye position in both yaw and pitch during approach periods is more centered around zero.
(C) Yaw eye positions between the two eyes, where blue and green points represent non-approach and approach time points, respectively.
(D) Proportion of congruent (moving the same yaw direction) and incongruent (moving in opposing yaw directions) eye movements during non-approach and approach times. Bars represent mean ± SEM (paired t-test; $p_{congruent}$<.0001; $p_{convergent}$ =.0016, $p_{divergent}$<.001).
(E) Difference in yaw position between the two eyes is significantly closer zero during approach periods (paired t-test, p<.001).
(F) Cross-correlation of change in bilateral eye position for both yaw and pitch for non-approach and approach periods.

Cross-correlations of changes in eye position between the two eyes revealed that the two eyes are positively correlated in yaw, but negatively correlated in pitch, consistent with stabilization from changes in pitch and roll of the head, and that these relationships were stronger during approaches (Figure 2E). Because measurements of head position were made with 2D videography, we could not directly measure changes in pitch and roll of the head, though these movements may contribute to the incongruent movements we see across the eyes (Wallace et al., 2013). As such, the observed reduction in incongruent eye movements could arise if there are fewer yaw head rotations during approach periods, in which case less VOR compensation would need to occur. Next, we aimed to understand the coordination of head and eye movements during approach behavior.

Horizontal eye movements are compensatory for yaw head rotations

The overall distribution of the change in head angles did not change during approaches (paired t-test, p=.46; Figure 3A), suggesting that head was not more centered in yaw during approaches. As such, the congruence between the two eyes during approaches can be averaged to give the overall eye position regardless of influence from roll or pitch. Averaging the yaw eye positions across the two eyes resulted in no difference in the distributions of yaw and pitch eye angles (Figure 3B; paired t-test, p_{yaw} = .93, p_{pitch}=.95). When the head was still, the eye position also did not change, where ~96.5% of non-approach and ~94% of approach time points fall within less than a 5 degree change (Figure 3C). This result suggests that most eye movements in the

horizontal axis in mice are driven by changes in head position.

Change in head angle was accompanied by opposing changes in eye yaw across both eyes, again consistent with relationships predicted by VOR-stabilization, though these distributions were quite variable (Figure 3D). More specifically, change in eye yaw had generally a negative relationship with change in head yaw, though there was a large spread. Interestingly, the strength of these correlations was slightly stronger during approach epochs and changes in eye theta were positively correlated with changes in head theta at - ~100 ms, suggesting that changes in head angle predict short-duration congruent changes in eye yaw during approaches (Figure 3E).

Head and gaze dynamics are driven by azimuth relative to cricket

To further examine these movements, we analyzed the dynamics of head movements and gaze during prey capture behavior. We calculated the gaze position, which is the sum of head and eye angles in yaw and reflects where in space, in egocentric coordinates, the animals are looking (Figure 4A, Figure 4B). Interestingly, gaze position had two distinct phases both during non-approach and approach epochs, the first of which consisted of large, congruent head and eye movements that led to sharp changes in gaze (ie., saccades). The second phase consisted of incongruent eye and head movements, as predicted by VOR, which effectively fixed the gaze to head movements (i.e., gaze stabilization; Figure 4A, Figure 4B).

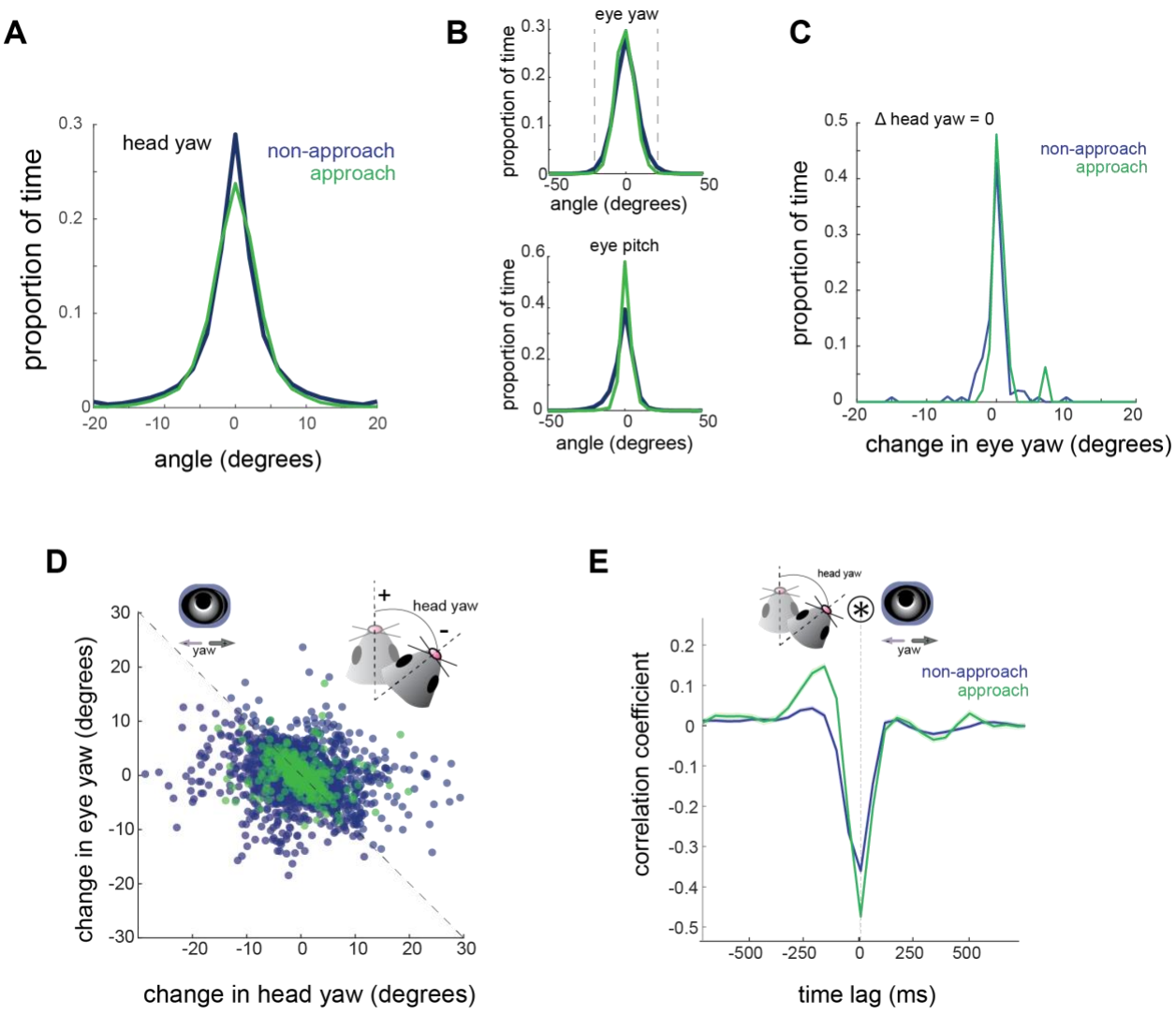

Figure 7. Horizontal eye movements are mostly compensatory for yaw head rotations.

(A) Overall distribution of changes in head angle do not differ between non-approach and approach periods (paired t-test, p=.46; n_{trials}=302; $n_{animals}$ =8).
(B) Distributions of yaw and pitch positions of the two eyes were not different during approach epochs (paired t-test, p_{yaw} = .93, p_{pitch}=.9). Dotted lines in eye yaw represent a 40 degree binocular zone.
(C)Distribution of change in horizontal eye angle when head is still (i.e., change in head yaw is zero), where ~96.5% of non-approach and ~94% of approach time points fall within less than a 5 degree change.
(D) Scatter plot of change in head yaw and changes in yaw for average of R and L eyes
(E) Cross-correlation between change in head yaw and change in eye yaw for approach and non-approach periods

The amplitude of the saccadic portions of congruent eye/head movement that shifted the gaze to a new relative position was small during approach periods, demonstrated by a higher frequency of low-amplitude head rotations for approach relative to non-approach periods (Figure 4C, 4D; <.0001). Higher-amplitude changes in head position, instead, were more frequent during non-approach periods (Figure 4C, 4D; p<.0001). This pattern suggests that during non-approaches animals may make large movements to orient towards prey, whereas during approaches, smaller shifts in head angle are used to reset and recalibrate the gaze over the target during locomotion.

We next sought to determine if these approach movements were directed towards the visual target (i.e., the cricket). Azimuth during approaches predicted changes in head yaw (Figure 4E), suggesting that movements towards the cricket during hunting were directed and non-random. Correspondingly, azimuth also predicted changes in eye yaw, and thus changes in gaze position (Figure 4F).

Together, these results suggest that to track visual objects under goal-directed contexts that require locomotion, mice use directed head movements and corresponding eye movements for resetting of gaze and gaze stabilization over the target during movement.

DISCUSSION

Using a set of miniaturized cameras, we investigated the coordination of eye and head movements during a visually guided and ethologically relevant behavior in mice,

approach and capture of live insect prey. We find that mice stabilize their gaze in front of them during approach periods and that this is achieved through utilization of quick saccadic head and eye movements and VOR stabilizing mechanisms.

Upon head rotation, we found saccadic eye and head movements, where both head and eye translations in yaw dimensions moved congruently, suggesting transient disengagement of VOR mechanisms, such that the eyes rapidly follow the direction of the head and reset the gaze to the new location. These saccadic movements are present in invertebrates and both foveate and
non-foveate vertebrates (reviewed in Land 1999) and work to recalibrate the relative position of gaze as animals turn. This brief period of congruent head and eye movements precedes a longer duration (~300 ms) period of horizontal recentering of eye position which stabilizes the gaze on the new target location as the head rotates during prey pursuit. This strategy, appropriately termed 'saccade and fixate' (Reviewed in Land, 2019) effectively fixes the binocular field like a spotlight over the target during locomotion while mice pursue prey.

Interestingly, there seem to be two distinct types of head saccade-like movements that may be involved in different aspects of the behavior. First, during orienting, prior to approach, large amplitude changes in head angle select the target to approach. Secondly, during approach periods while head rotation is more gradual and gaze is well stabilized with head position, we observed step-like shifts in gaze, that re-centered eye position, similar to in the optokinetic response when the eyes track a moving stimulus.

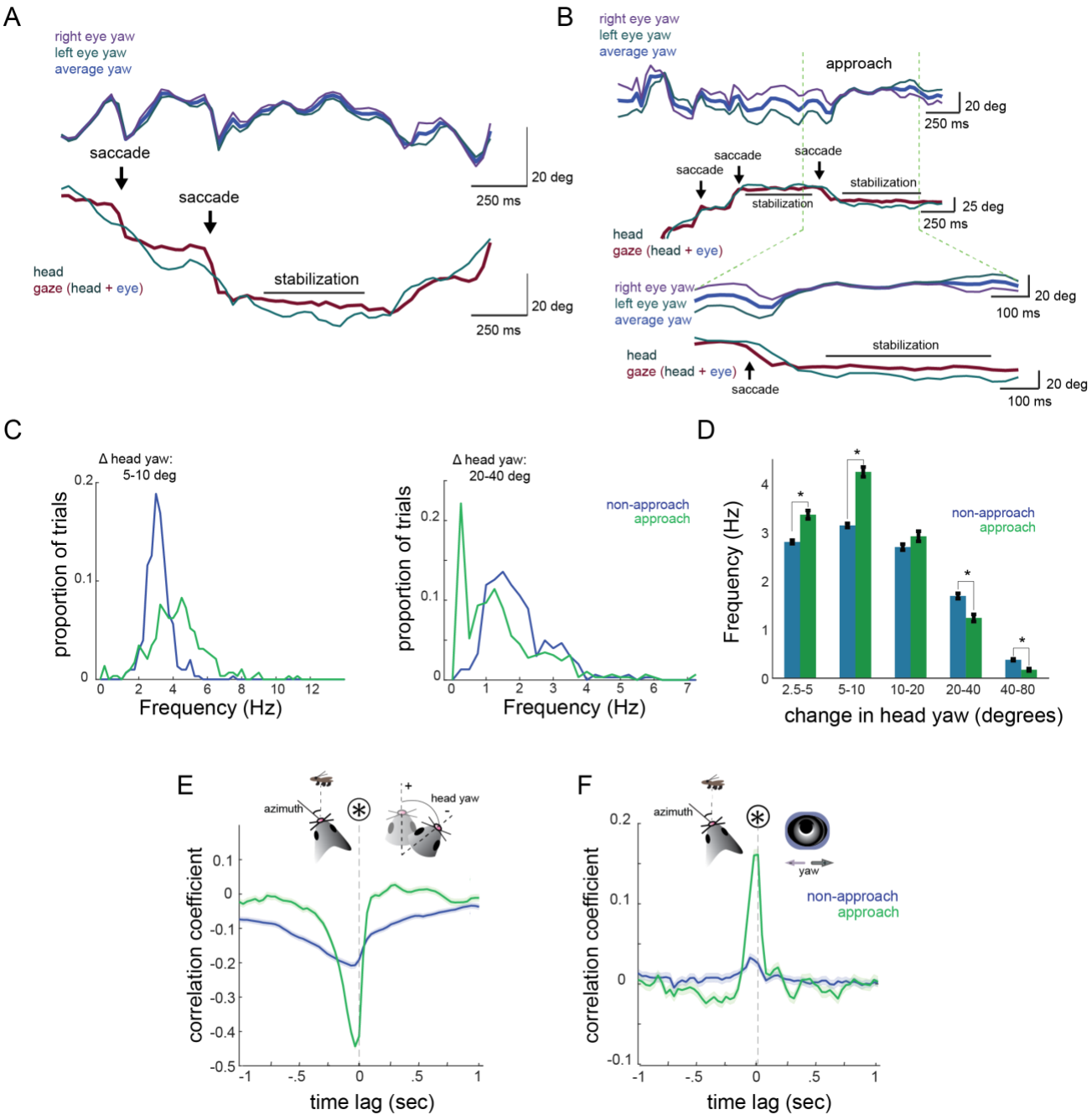

Figure 8: Head movements are directed towards cricket during hunting.
(A) An example trace of gaze, the sum of eye and head yaw, which shows periods of quick shifts in the direction of the head (saccades) and stabilization where gaze position closely matches the head angle. Small changes in gaze during the stabilization period work to recalibrate the gaze position to the head during locomotion.
(B) An example of gaze before and during an approach period. Note the centering of the two eyes after approach begins.

(C) The frequency for small amplitude changes (between 5-10 degrees) in head yaw is higher during approach periods. In contrast, for higher amplitude changes in head angle

(between 20-40 degrees), the frequency is higher during non-approach periods ($p_{5-10}<.0001$; $p_{20-40}<.0001$).
(D) The average frequency of small amplitude (2.5-10 degrees) shifts in head yaw is higher during approaches. For high amplitude changes (20-80 degrees), the frequency is higher during non-approach periods (paired t-test, $p_{2.5-5}<.0001$, $p_{5-10}<.0001$, $p_{10-20}= .66$, $p_{20-40}<.0001$, $p_{40-80}<.0001$).
(E) Cross-correlation of azimuth (the horizontal angle to the cricket) and changes in head yaw. Azimuth predicts changes in head yaw.
(F) Cross-correlation of azimuth and eye yaw shows that azimuth predicts changes in eye yaw.

In this study, we observed that roughly half of eye movements in mice are bilaterally incongruent during non-approach periods. During approach periods, however, the two eyes center and become congruent in their movements, suggesting more coordination across the two eyes. Incongruence of eye movements is thought to arise from motion of the animal, as it is seen much less in head-restrained mice (Payne and Raymond 2017). We believe this incongruence may be due to changes in roll of the head, rather than yaw, which has been reported before (Wallace et al. 2013), where roll of the head leads to both divergent and convergent eye movements. Though some afoveate species use independent and incongruent eye movements for visual sampling, because we see very little change in eye position when the head is stationary, mice likely do not use this strategy.

Though mice do not have foveae, they may have an enhanced binocular visual space representation due to different densities of alpha RGCs (Bleckert et al., 2014), and have enhanced contrast detection in the binocular, as opposed to monocular fields (Speed et al. 2019). Together, this may suggest a fovea-like representation where visual objects of interest are probable in central positions. In the present study we observed that eye

position was more centralized during approach periods. For mice, this may be the position at which there is the most monocular overlap, or widest binocular field. Additionally, we find that eye position mostly falls within the 40 degree binocular zone (Figure 3B).

Regardless of foveae, in the case of prey capture behavior, visual targets (i.e., crickets) may quickly move between binocular and monocular areas of the visual field, requiring a strategy to maintain visual a stable binocular field. We find that this occurs through directed head movements and corresponding resetting and stabilizing eye movements. A benefit of this strategy is that it reduces image blur from surrounding motion by centering the visual field over the retina and stabilizing gaze during locomotion.

To our knowledge, this study is one of the first to record eye movements in freely moving rodents (Wallace et al. 2013; Payne and Raymond 2017; Meyer et al. 2018) and the first to do so during an ethologically relevant behavior. Though similar findings have been reported in other species, this is the first to show saccadic resetting and gaze stabilization during locomotion in mice, particularly under a visual goal directed context. This work will provide a basis for future studies of visuomotor behaviors and visual processing in the context of self-motion in more naturalistic contexts.

CHAPTER IV

CONCLUSIONS

In this dissertation, I presented results from two main projects centered around contextual modulation of vision and how the nervous system allow organisms to interact within their environments. The first of these, presented in Chapter II, is focused on contextual modulation by a neuromodulatory receptor subsystem, the serotonin-2A system, which we found to important in balancing internal and external information streams within the cortex. When the serotonin-2A ($5HT_{2A}$) subsystem is overactive, the processing of external visual stimuli is dramatically reduced, suggesting an over-weighting of internal representations and expectations, which could give rise to hallucinations. This particular study was the first to examine this process at a neurophysiological in awake animals, rather than the cognitive or psychophysical, level and provides a basis for the study of circuit-specific actions of $5HT_{2A}$ modulation on cortical function. For example, since we have determined that $5HT_{2A}$ activation reduces sensory drive, future studies can determine if this is due to a reduction in activity at lower levels of the visual hierarchy (i.e., retina or LGN) or if feedback projections from higher-order cortical areas somehow inhibit V1 activity.

The second of the two projects presented in this dissertation is focused on visuomotor behavior during a goal directed task that requires vision. By devising a system to bilaterally record eye movements, I found that non-foveate animals can still accomplish visual tasks when objects of interest are in the center of the visual field. The oculomotor strategy used combines two main behaviors, the first of which is directed

head movements, yoked to congruent eye movements, which creates large gaze shifts, characteristic of saccades. This occurs during visual target selection and also, with a smaller amplitude, during visual target pursuit. These resetting eye movements which occur during target pursuit are similar to eye movements generated by the optokinetic reflex (OKR) that occurs from viewing motion-stimuli. The next behavior is stabilization of gaze, which occurs through VOR-like stabilizing movements, where eye movements compensate for any head movements; this stabilizes the gaze relative to head movements. Together, these results display an oculomotor strategy that combines both OKR and VOR-type mechanisms. This has not been shown before in freely behaving rodents, but is observed in fish and crabs (Land, 1999).

In this project, I discovered that during self-motion, saccadic eye movements are achieved thorough congruent movement with the head. Depending on the magnitude of head turns, we discovered two main types of saccades: target selection saccades and re-centering saccades. Target selection saccades occur during rapid head turns, and work to establish a new gaze position over the visual target. In contrast, re-setting saccades occur during longer duration and magnitude turns that are constant. In these cases, the eyes move rapidly in the direction of the head turn until they reach their maximum position (i.e., for a left head turn, the left eye moves laterally and the right eye moves nasally), then slowly shift opposite the head, back to their centralized position, effectively stabilizing the gaze. These resetting saccades are thus interleaved by periods of compensatory eye movements. By definition, compensatory eye movements occur through incongruence of eye and head movements.

This work will be the basis of future studies of visual processing in more natural contexts. For example, this freely moving eye tracking method can be combined with electrophysiology or imaging to understand modulation of neural activity by gaze position. In addition, adding an outward facing camera that records the visual scene from the mouse's point of view can be used in conjunction with an eye tracking camera and neural recording methods to understand visual feature encoding in a context more realistic than gaze and head-fixation. By shifting the visual scene recorded from the outward facing camera by the change in eye position, one can calculate the visual stimulus that the mouse encountered, then apply analysis methods such as spike-triggered-averaging to observe natural receptive fields and their modulation by behavioral states.

One of the interesting findings in this study is the reduction of incongruent eye movements during approach periods. Though this finding strongly suggests that mice are essentially locking their gaze centrally, this arises from a reduction in pitch and roll of head movements, which were measured with an accelerometer and gyroscope. This suggests that the strategy used by mice is not just stabilization of gaze through compensatory eye movements, but that this is achieved by stabilization of the head as well. To clarify this aspect prey capture behavior, a gyroscope which records angular position in all dimensions (pitch, roll, and yaw) would provide the most temporally and spatially precise measurements. I have completed these experiments and they will be added to an upcoming publication centered on Chapter III of this dissertation.

Additionally, this particular behavior is mediated by the lateral superior colliculus, where the response of specific cell types to particular visual features drive orienting and approach of the mouse towards the cricket (Hoy et al., 2019). Superior colliculus is functionally modulated by cortical projections from primary visual cortex (V1; Ahmadlou et al., 2018). One of the functions of cortex is integrating contextually relevant information during complex tasks. If the prey capture assay was more complex (i.e., required navigation, avoidance of obstacles, or computations of figure-ground segmentation), V1 may contribute to the behavior by modulating superior colliculus activity. Using optogenetic shutdown of V1 in a complex and more natural environment, we are beginning to assess the role of cortical modulation in prey capture behavior.

Performing an optogenetic shutdown through activation of channelrhodopsin-2 expressing Parvalbumin (PV) inhibitory neurons in V1, we have found that V1 becomes recruited into this task when the prey capture arena is more complex. There is a slight deficit in time to successful capture when a noise background wallpaper is added to the walls of the arena. When physical obstacles are added (stacks of lego blocks) in addition to the noise background, there is a dramatic deficit in hunting ability, where animals take roughly four times longer to successfully capture a cricket.

Together, my work has examined the process of vision from two different angles and has laid the groundwork for the future study of two different aspects of contextual visual processing: the balancing of internal/external representations and the influence of

self-motion on visual processing and behavior. As a whole, the driving question behind the two described projects was focused on understanding how the brain allows us to interact in the world. In Chapter III, I described this process at the input stage, by investigating the coordination of eye and head movements during a visually guided and goal directed behavior that requires visual sampling. In Chapter II, centered on the processing step, I investigated the integration of external and internal information, and its disruption through $5HT_{2A}$ receptor signaling.

Though these two projects were conducted separately, each answered long-standing questions in the field of visual neuroscience: how do non-foveate animals track visual targets, and how does $5HT_{2A}$ receptor signaling affect visual processing. The two together have created a deeper understanding of input and processing stages of visual interactions with the world.

APPENDICES

Supplementary Materials for Chapter II

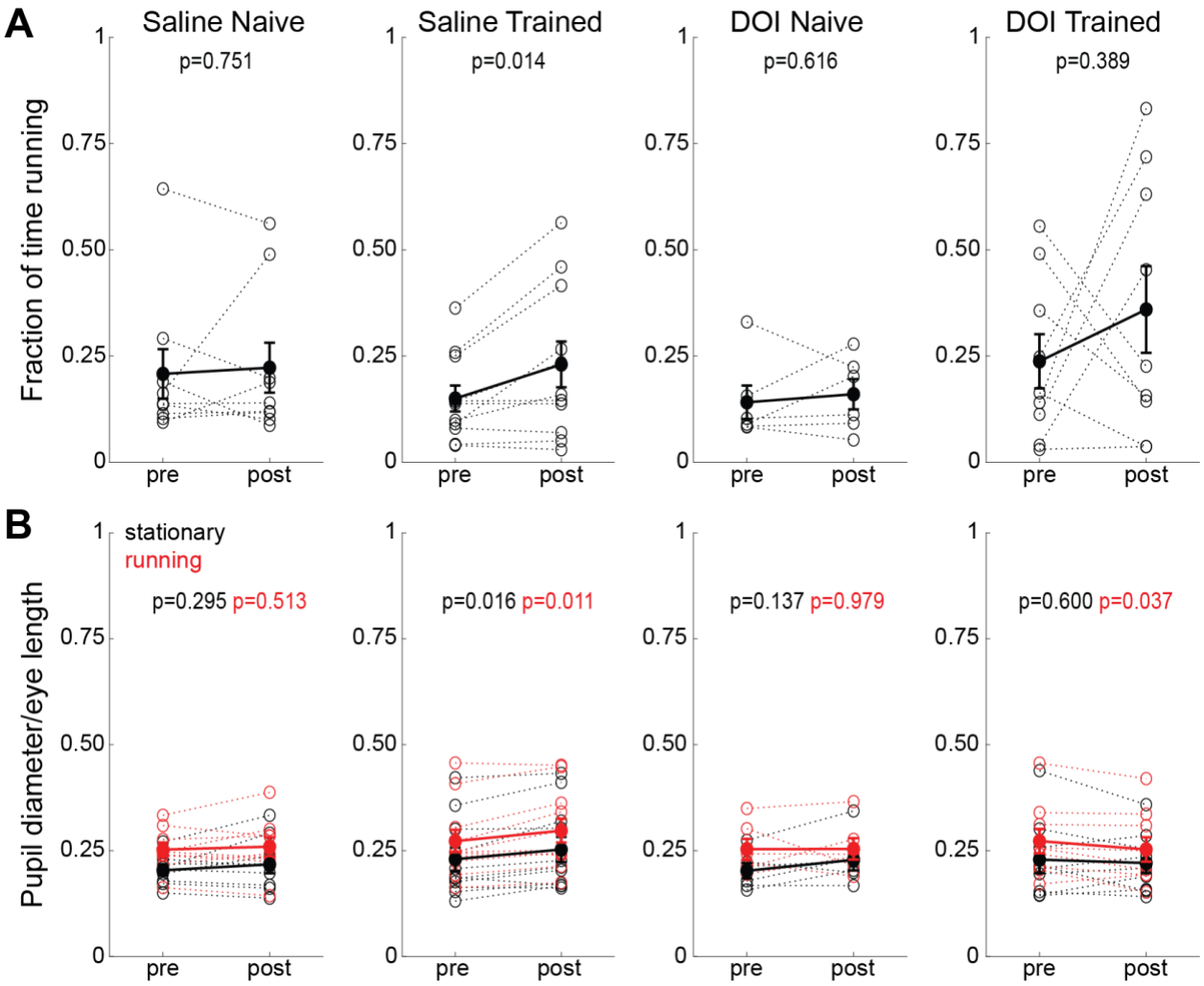

Supplementary Figure S1: Baseline and post-drug measures relating to behavioral state.
(A) Total fraction of experiment time spent running before (pre) and after (post) administration of saline or DOI for each group. Open circles connected by dotted lines represent individual animals and closed circles connected by thick lines with error bars are group mean ± SEM. Significance from paired t-tests are reported above each group plot.
(B) Average pupil diameter normalized to length of the animal's eye (both measured in pixels) before and after drug administration. Black data represent stationary and red represent running periods. Open circles connected by dotted lines represent individual animals and close circles connected by thick lines with error bars are group mean ± SEM.

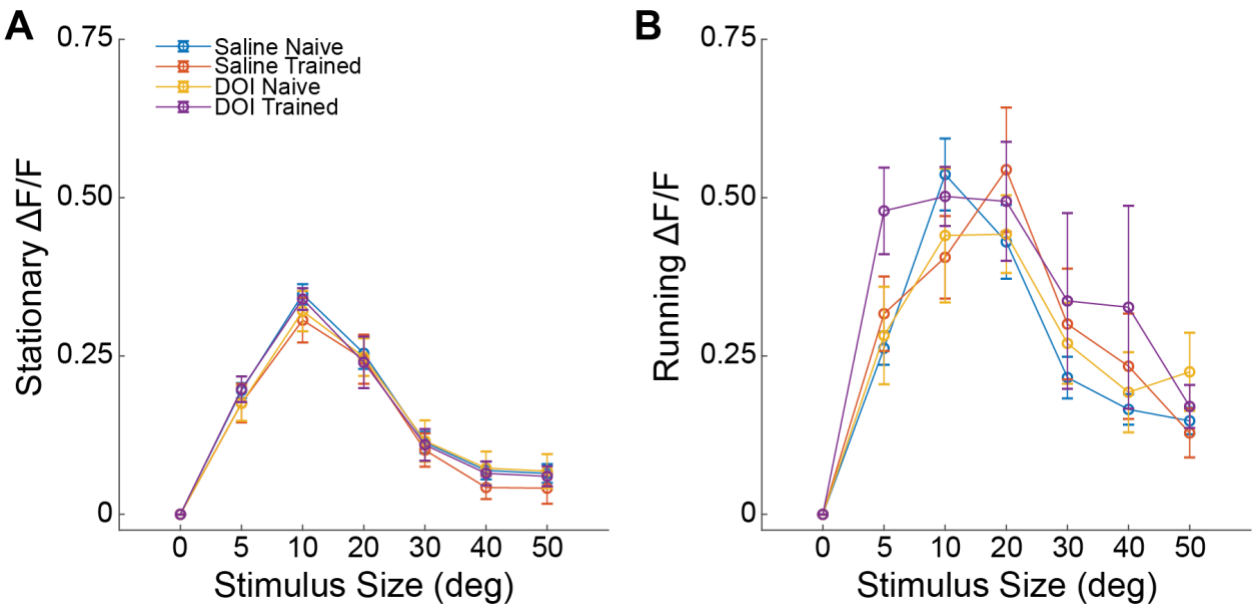

Supplementary Figure S2: Comparison of baseline response magnitudes across experimental groups.
Size tuning curves showing baseline response magnitudes (before drug application) of all four groups for (A) stationary, and (B) running periods ($p = 0.619$ stationary, $p = 0.939$ running, Kruskal-Wallis). Open circles are group means and error bars are SEM.

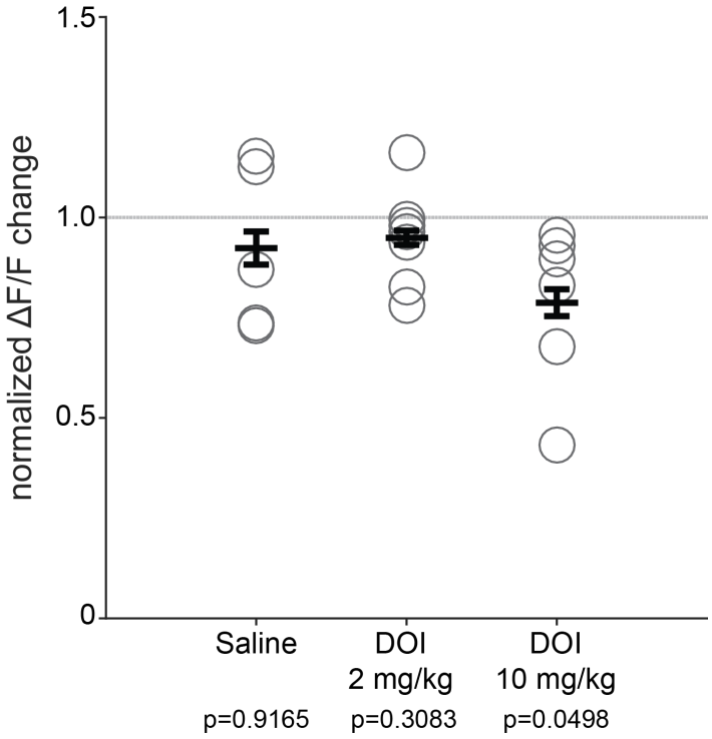

Supplementary Figure S3: Comparison of DOI dose and change in widefield response magnitude in naive animals. Comparison of changes to visually evoked responses after drug administration across groups of naive animals (as in Figure 1D-F). Open circles are individual animals, bars are mean ± SEM. A value of 1 represents no change, p-values are two-tailed paired t-test for pre vs. post within group.

REFERENCES CITED

Abraham, H. D., and E. Wolf. 1988. “Visual Function in Past Users of LSD: Psychophysical Findings.” *Journal of Abnormal Psychology* 97 (4): 443–47.

Ahmadlou, Mehran, Larry S. Zweifel, and J. Alexander Heimel. 2018. “Functional Modulation of Primary Visual Cortex by the Superior Colliculus in the Mouse.” *Nature Communications* 9 (1): 3895.

Alhazen, and A. Mark Smith. 2001. *Alhacen’s Theory of Visual Perception: A Critical Edition, with English Translation and Commentary, of the First Three Books of Alhacen's De Aspectibus, the Medieval Latin Version of Ibn Al-Haytham's Kitab Al-Manazir*. American Philosophical Society.

Avesar, D. & Gulledge, A.T., 2012. Selective serotonergic excitation of callosal projection neurons. *Frontiers in neural circuits*, 6, p.12.
Ayaz, A. et al., 2013. Locomotion controls spatial integration in mouse visual cortex. *Current biology: CB*, 23(10), pp.890–894.

Baggott, Matthew J., Jennifer D. Siegrist, Gantt P. Galloway, Lynn C. Robertson, Jeremy R. Coyle, and John E. Mendelson. 2010. “Investigating the Mechanisms of Hallucinogen-Induced Visions Using 3,4-Methylenedioxyamphetamine (MDA): A Randomized Controlled Trial in Humans.” *PLoS ONE*. https://doi.org/10.1371/journal.pone.0014074.

Bleckert, Adam, Gregory W. Schwartz, Maxwell H. Turner, Fred Rieke, and Rachel O. L. Wong. 2014. “Visual Space Is Represented by Nonmatching Topographies of Distinct Mouse Retinal Ganglion Cell Types.” *Current Biology: CB* 24 (3): 310–15.

Brainard, D.H., 1997. The Psychophysics Toolbox. *Spatial vision*, 10(4), pp.433–436.

Burgess, Christian R., Rohan N. Ramesh, Arthur U. Sugden, Kirsten M. Levandowski, Margaret A. Minnig, Henning Fenselau, Bradford B. Lowell, and Mark L. Andermann. 2016. “Hunger-Dependent Enhancement of Food Cue Responses in Mouse Postrhinal Cortex and Lateral Amygdala.” *Neuron* 91 (5): 1154–69.

Butler, P. D., J. M. Harkavy-Friedman, X. F. Amador, and J. M. Gorman. 1996. “Backward Masking in Schizophrenia: Relationship to Medication Status, Neuropsychological Functioning, and Dopamine Metabolism.” *Biological Psychiatry* 40 (4): 295–98.

Butler, P.D., Silverstein, S.M. & Dakin, S.C., 2008. Visual perception and its impairment in schizophrenia. *Biological psychiatry*, 64(1), pp.40–47.

Carhart-Harris, R.L. et al., 2016. Neural correlates of the LSD experience revealed by multimodal neuroimaging. *Proceedings of the National Academy of Sciences of the United States of America*, 113(17), pp.4853–4858.

Carhart-Harris, R.L. & Goodwin, G.M., 2017. The Therapeutic Potential of Psychedelic Drugs: Past, Present, and Future. *Neuropsychopharmacology: official publication of the American College of Neuropsychopharmacology*, 42(11), pp.2105–2113.

Cartmill, M., 1974. Rethinking Primate Origins. *Science* New Series, Vol. 184, No. 4135 pp. 436-443.

Cartmill, Matt. 2005. "New Views on Primate Origins." *Evolutionary Anthropology: Issues, News, and Reviews*. https://doi.org/10.1002/evan.1360010308.

Carlsson, M., and A. Carlsson. 1990. "Schizophrenia: A Subcortical Neurotransmitter Imbalance Syndrome?" *Schizophrenia Bulletin*. https://doi.org/10.1093/schbul/16.3.425.

Carter, Olivia L., Felix Hasler, John D. Pettigrew, Guy M. Wallis, Guang B. Liu, and Franz X. Vollenweider. 2007. "Psilocybin Links Binocular Rivalry Switch Rate to Attention and Subjective Arousal Levels in Humans." *Psychopharmacology* 195 (3): 415–24.

Cassidy, C.M. et al., 2018. A Perceptual Inference Mechanism for Hallucinations Linked to Striatal Dopamine. *Current biology: CB*, 28(4), pp.503–514.e4.

Celada, P. et al., 2008. The hallucinogen DOI reduces low-frequency oscillations in rat prefrontal cortex: reversal by antipsychotic drugs. *Biological psychiatry*, 64(5), pp.392–400.

Clark, Benjamin J., Derek A. Hamilton, and Ian Q. Whishaw. 2006. "Motor Activity (exploration) and Formation of Home Bases in Mice (C57BL/6) Influenced by Visual and Tactile Cues: Modification of Movement Distribution, Distance, Location, and Speed." *Physiology & Behavior* 87 (4): 805–16.

Dadarlat, Maria C., and Michael P. Stryker. 2017. "Locomotion Enhances Neural Encoding of Visual Stimuli in Mouse V1." *The Journal of Neuroscience: The Official Journal of the Society for Neuroscience* 37 (14): 3764–75.

Dawkins, Marian Stamp. 2002. "What Are Birds Looking at? Head Movements and Eye Use in Chickens." *Animal Behaviour*. https://doi.org/10.1006/anbe.2002.1999.

Dimpfel, W., Spüler, M. & Nichols, D.E., 1989. Hallucinogenic and stimulatory amphetamine derivatives: fingerprinting DOM, DOI, DOB, MDMA, and MBDB by spectral analysis of brain field potentials in the freely moving rat (Tele-Stereo-EEG). *Psychopharmacology*, 98(3), pp.297–303.

Dombeck, D.A. et al., 2007. Imaging large-scale neural activity with cellular resolution in awake, mobile mice. *Neuron*, 56(1), pp.43–57.

Drager, U. C. 1978. “Observations on Monocular Deprivation in Mice.” *Journal of Neurophysiology*. https://doi.org/10.1152/jn.1978.41.1.28.

Dray, A. et al., 1980. The effects of LSD and some analogues on the responses of single cortical neurons of the cat to optical stimulation. *Brain research*, 200(1), pp.105–121.

Fiser, A. et al., 2016. Experience-dependent spatial expectations in mouse visual cortex. *Nature neuroscience*, 19(12), pp.1658–1664.

Frecska, E., K. D. White, and L. E. Luna. 2004. “Effects of Ayahuasca on Binocular Rivalry with Dichoptic Stimulus Alternation.” *Psychopharmacology* 173 (1-2): 79–87.

Fukushima, Kikuro, Junko Fukushima, Tateo Warabi, and Graham R. Barnes. 2013. “Cognitive Processes Involved in Smooth Pursuit Eye Movements: Behavioral Evidence, Neural Substrate and Clinical Correlation.” *Frontiers in Systems Neuroscience* 7 (March): 4.

Gegenfurtner, Karl R. 2016. “The Interaction Between Vision and Eye Movements.” *Perception* 45 (12): 1333–57.

Goda, S.A. et al., 2013. Serotonergic hallucinogens differentially modify gamma and high frequency oscillations in the rat nucleus accumbens. *Psychopharmacology*, 228(2), pp.271–282.

Gong, S. et al., 2007. Targeting Cre recombinase to specific neuron populations with bacterial artificial chromosome constructs. *The Journal of neuroscience: the official journal of the Society for Neuroscience*, 27(37), pp.9817–9823.

González-Maeso, Javier, Noelia V. Weisstaub, Mingming Zhou, Pokman Chan, Lidija Ivic, Rosalind Ang, Alena Lira, et al. 2007. “Hallucinogens Recruit Specific Cortical 5-HT(2A) Receptor-Mediated Signaling Pathways to Affect Behavior.” *Neuron* 53 (3): 439–52.

Green, M. F., and K. H. Nuechterlein. 1999. “Cortical Oscillations and Schizophrenia: Timing Is of the Essence.” *Archives of General Psychiatry*.

Grossberg, S., 2000. How hallucinations may arise from brain mechanisms of learning, attention, and volition. *Journal of the International Neuropsychological Society: JINS*, 6(5), pp.583–592.

Guerra-Doce, Elisa. 2015. “Psychoactive Substances in Prehistoric Times: Examining the Archaeological Evidence.” *Time and Mind*. https://doi.org/10.1080/1751696x.2014.993244.

Hanks, J.B. & González-Maeso, J., 2013. Animal models of serotonergic psychedelics. *ACS chemical neuroscience*, 4(1), pp.33–42.

Harris, K.D. et al., 2000. Accuracy of tetrode spike separation as determined by simultaneous intracellular and extracellular measurements. *Journal of neurophysiology*, 84(1), pp.401–414.

Hensler, Julie G. 2012. “Serotonin.” *Basic Neurochemistry*. https://doi.org/10.1016/b978-0-12-374947-5.00015-8.

Hirota, J. & Shimizu, S., 2012. Routes of Administration. In *The Laboratory Mouse*. pp. 709–725.

Homann, J. et al., 2017. Predictive Coding of Novel versus Familiar Stimuli in the Primary Visual Cortex. Available at: http://dx.doi.org/10.1101/197608.

Hoy, Jennifer L., Hannah I. Bishop, and Cristopher M. Niell. n.d. “Defined Cell Types in Superior Colliculus Make Distinct Contributions to Prey Capture Behavior in the Mouse.” https://doi.org/10.1101/626622.

Hoy, Jennifer L., Iryna Yavorska, Michael Wehr, and Cristopher M. Niell. 2016. “Vision Drives Accurate Approach Behavior during Prey Capture in Laboratory Mice.” *Current Biology: CB* 26 (22): 3046–52.

Hoy, J.L. & Niell, C.M., 2015. Layer-specific refinement of visual cortex function after eye opening in the awake mouse. *The Journal of neuroscience: the official journal of the Society for Neuroscience*, 35(8), pp.3370–3383.

Huberman, Andrew D., and Cristopher M. Niell. 2011. “What Can Mice Tell Us about How Vision Works?” *Trends in Neurosciences* 34 (9): 464–73.

Jia, X., Tanabe, S. & Kohn, A., 2013. Gamma and the Coordination of Spiking Activity in Early Visual Cortex. *Neuron*, 77(4), pp.762–774.

Johnson, M.W. & Griffiths, R.R., 2017. Potential Therapeutic Effects of Psilocybin. *Neurotherapeutics: the journal of the American Society for Experimental NeuroTherapeutics*, 14(3), pp.734–740.

Kalatsky, V.A. & Stryker, M.P., 2003. New paradigm for optical imaging: temporally encoded maps of intrinsic signal. *Neuron*, 38(4), pp.529–545.

Khan, Adil G., and Sonja B. Hofer. 2018. “Contextual Signals in Visual Cortex.” *Current Opinion in Neurobiology* 52 (October): 131–38.

Knight, A.R. et al., 2004. Pharmacological characterisation of the agonist radioligand binding site of 5-HT(2A), 5-HT(2B) and 5-HT(2C) receptors. *Naunyn-Schmiedeberg's archives of pharmacology*, 370(2), pp.114–123.

Kometer, M. et al., 2013. Activation of serotonin 2A receptors underlies the psilocybin-induced effects on α oscillations, N170 visual-evoked potentials, and visual hallucinations. *The Journal of neuroscience: the official journal of the Society for Neuroscience*, 33(25), pp.10544–10551.

Land, M. F. 1999. "Motion and Vision: Why Animals Move Their Eyes." *Journal of Comparative Physiology. A, Sensory, Neural, and Behavioral Physiology* 185 (4): 341–52.

Land, Michael. 2019. "Eye Movements in Man and Other Animals." *Vision Research* 162 (September): 1–7.

Liechti, M.E., 2017. Modern Clinical Research on LSD. *Neuropsychopharmacology: official publication of the American College of Neuropsychopharmacology*, 42(11), pp.2114–2127.

Lopes, Gonçalo, Niccolò Bonacchi, João Frazão, Joana P. Neto, Bassam V. Atallah, Sofia Soares, Luís Moreira, et al. 2015. "Bonsai: An Event-Based Framework for Processing and Controlling Data Streams." *Frontiers in Neuroinformatics* 9 (April): 7.

Mathis, Alexander, Pranav Mamidanna, Kevin M. Cury, Taiga Abe, Venkatesh N. Murthy, Mackenzie Weygandt Mathis, and Matthias Bethge. 2018. "DeepLabCut: Markerless Pose Estimation of User-Defined Body Parts with Deep Learning." *Nature Neuroscience* 21 (9): 1281–89.

Meyer, Arne F., Jasper Poort, John O'Keefe, Maneesh Sahani, and Jennifer F. Linden. 2018. "A Head-Mounted Camera System Integrates Detailed Behavioral Monitoring with Multichannel Electrophysiology in Freely Moving Mice." *Neuron* 100 (1): 46–60.e7.

Mitra, P. & Bokil, H., 2007. *Observed Brain Dynamics*, Oxford University Press.

Mitra, P.P. & Pesaran, B., 1999. Analysis of dynamic brain imaging data. *Biophysical journal*, 76(2), pp.691–708.

Moran, L.V. & Hong, L.E., 2011. High vs low frequency neural oscillations in schizophrenia. *Schizophrenia bulletin*, 37(4), pp.659–663.

Morris, Adam P., and Bart Krekelberg. 2019. "A Stable Visual World in Primate Primary Visual Cortex." *Current Biology: CB* 29 (9): 1471–80.e6.

Morris, Richard G. M. 1981. “Spatial Localization Does Not Require the Presence of Local Cues.” *Learning and Motivation*. https://doi.org/10.1016/0023-9690(81)90020-5.

Nichols, D.E., 2016. Psychedelics. *Pharmacological reviews*, 68(2), pp.264–355.

Niell, C.M. & Stryker, M.P., 2008. Highly selective receptive fields in mouse visual cortex. *The Journal of neuroscience: the official journal of the Society for Neuroscience*, 28(30), pp.7520–7536.

Niell, C.M. & Stryker, M.P., 2010. Modulation of visual responses by behavioral state in mouse visual cortex. *Neuron*, 65(4), pp.472–479.

Payne, Hannah L., and Jennifer L. Raymond. 2017. “Magnetic Eye Tracking in Mice.” *eLife* 6 (September). https://doi.org/10.7554/eLife.29222.

Pelli, D.G., 1997. The VideoToolbox software for visual psychophysics: transforming numbers into movies. *Spatial vision*, 10(4), pp.437–442.

Phillips, W.A. & Silverstein, S.M., 2013. The coherent organization of mental life depends on mechanisms for context-sensitive gain-control that are impaired in schizophrenia. *Frontiers in psychology*, 4, p.307.

Pnevmatikakis, E.A. et al., 2016. Simultaneous Denoising, Deconvolution, and Demixing of Calcium Imaging Data. *Neuron*, 89(2), pp.285–299.

Porter, W.P. et al., 1985. A comparison of subcutaneous and intraperitoneal oxytetracycline injection methods for control of infectious disease in the rat. *Laboratory animals*, 19(1), pp.3–6.

Preller, K.H. et al., 2018. Changes in global and thalamic brain connectivity in LSD-induced altered states of consciousness are attributable to the 5-HT2A receptor. *eLife*, 7. Available at: http://dx.doi.org/10.7554/eLife.35082.

Ringach, D.L., Hawken, M.J. & Shapley, R., 1997. Dynamics of orientation tuning in macaque primary visual cortex. *Nature*, 387(6630), pp.281–284.

Rose, D. & Horn, G., 1977. Effects of LSD on the response of single units in cat visual cortex. *Experimental brain research. Experimentelle Hirnforschung. Experimentation cerebrale*, 27(1), pp.71–80.

Sacks, Oliver. 2012. *Hallucinations*. Vintage.

Saleem, Aman B., E. Mika Diamanti, Julien Fournier, Kenneth D. Harris, and Matteo Carandini. 2018. “Coherent Encoding of Subjective Spatial Position in Visual Cortex and Hippocampus.” *Nature* 562 (7725): 124–27.

Schindler, E.A.D. et al., 2012. Serotonergic and dopaminergic distinctions in the behavioral pharmacology of (±)-1-(2,5-dimethoxy-4-iodophenyl)-2-aminopropane (DOI) and lysergic acid diethylamide (LSD). *Pharmacology, biochemistry, and behavior*, 101(1), pp.69–76.

Schmidt, C.J. et al., 1995. The role of 5-HT2A receptors in antipsychotic activity. *Life sciences*, 56(25), pp.2209–2222.

Schmitzer-Torbert, N. et al., 2005. Quantitative measures of cluster quality for use in extracellular recordings. *Neuroscience*, 131(1), pp.1–11.

Sedley, W. & Cunningham, M.O., 2013. Do cortical gamma oscillations promote or suppress perception? An under-asked question with an over-assumed answer. *Frontiers in human neuroscience*, 7, p.595.

Seillier, L. et al., 2017. Serotonin Decreases the Gain of Visual Responses in Awake Macaque V1. *The Journal of neuroscience: the official journal of the Society for Neuroscience*, 37(47), pp.11390–11405.

Shuler, Marshall G., and Mark F. Bear. 2006. "Reward Timing in the Primary Visual Cortex." *Science* 311 (5767): 1606–9.
Shulgin, A. & Shulgin, A., 1991. *Pihkal: A Chemical Love Story*, Berkeley, CA: Transform Press.

Sirota, A. et al., 2008. Entrainment of neocortical neurons and gamma oscillations by the hippocampal theta rhythm. *Neuron*, 60(4), pp.683–697.

Speed, Anderson, Joseph Del Rosario, Christopher P. Burgess, and Bilal Haider. 2019. "Cortical State Fluctuations across Layers of V1 during Visual Spatial Perception." *Cell Reports* 26 (11): 2868–74.e3.

Stănişor, Liviu, Chris van der Togt, Cyriel M. A. Pennartz, and Pieter R. Roelfsema. 2013. "A Unified Selection Signal for Attention and Reward in Primary Visual Cortex." *Proceedings of the National Academy of Sciences of the United States of America* 110 (22): 9136–41.

Stephens, E.K., Avesar, D. & Gulledge, A.T., 2014. Activity-dependent serotonergic excitation of callosal projection neurons in the mouse prefrontal cortex. *Frontiers in neural circuits*, 8, p.97.

Tibber, M.S. et al., 2013. Visual surround suppression in schizophrenia. *Frontiers in psychology*, 4, p.88.

Turner, P.V., Pekow, C., et al., 2011. Administration of substances to laboratory animals: equipment considerations, vehicle selection, and solute preparation. *Journal of the American Association for Laboratory Animal Science: JAALAS*, 50(5), pp.614–627.

Turner, P.V., Brabb, T., et al., 2011. Administration of substances to laboratory animals: routes of administration and factors to consider. *Journal of the American Association for Laboratory Animal Science: JAALAS*, 50(5), pp.600–613.

Uhlhaas, P.J. & Singer, W., 2010. Abnormal neural oscillations and synchrony in schizophrenia. *Nature reviews. Neuroscience*, 11(2), pp.100–113.

Vollenweider, F.X. et al., 1998. Psilocybin induces schizophrenia-like psychosis in humans via a serotonin-2 agonist action. *Neuroreport*, 9(17), pp.3897–3902.

Wallace, Damian J., David S. Greenberg, Juergen Sawinski, Stefanie Rulla, Giuseppe Notaro, and Jason N. D. Kerr. 2013. "Rats Maintain an Overhead Binocular Field at the Expense of Constant Fusion." *Nature* 498 (7452): 65–69.

Watakabe, A. et al., 2009. Enriched expression of serotonin 1B and 2A receptor genes in macaque visual cortex and their bidirectional modulatory effects on neuronal responses. *Cerebral cortex* , 19(8), pp.1915–1928.

Weber, E.T. & Andrade, R., 2010. Htr2a Gene and 5-HT(2A) Receptor Expression in the Cerebral Cortex Studied Using Genetically Modified Mice. *Frontiers in neuroscience*, 4. Available at: http://dx.doi.org/10.3389/fnins.2010.00036.

Wekselblatt, J.B. et al., 2016. Large-scale imaging of cortical dynamics during sensory perception and behavior. *Journal of neurophysiology*, 115(6), pp.2852–2866.

Weyand, T. G., and J. G. Malpeli. 1993. "Responses of Neurons in Primary Visual Cortex Are Modulated by Eye Position." *Journal of Neurophysiology* 69 (6): 2258–60.

Wood, J., Kim, Y. & Moghaddam, B., 2012. Disruption of prefrontal cortex large scale neuronal activity by different classes of psychotomimetic drugs. *The Journal of neuroscience: the official journal of the Society for Neuroscience*, 32(9), pp.3022–3031.

Yarbus, Alfred L. 1967. "Saccadic Eye Movements." *Eye Movements and Vision*. https://doi.org/10.1007/978-1-4899-5379-7_5.

Zenger-Landolt, B. & Heeger, D.J., 2003. Response suppression in v1 agrees with psychophysics of surround masking. *The Journal of neuroscience: the official journal of the Society for Neuroscience*, 23(17), pp.6884–6893.

Zirkle, Conway. (1941). *Natural Selection Before the 'Origin of Species'*. Proceedings of the American Philosophical Association 84: 71-123.